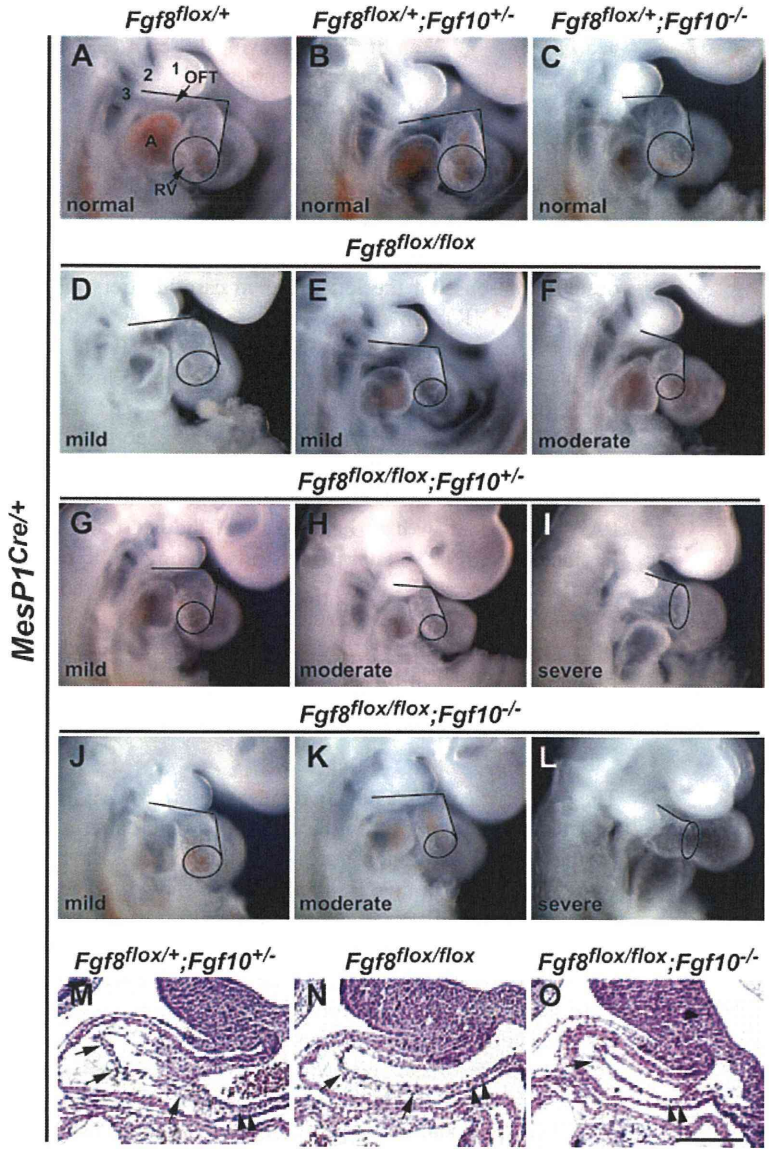

Figure 1. OFT and RV morphology of E9.5 *Fgf8;Fgf10;MesP1Cre* compound mutants. A through L, Right lateral views of embryos are shown, and genotypes are listed above the images. In $Fgf8^{flox/+}$ (A), $Fgf8^{flox/+};Fgf10^{+/-}$ (B), and $Fgf8^{flox/+};Fgf10^{-/-}$ (C) embryos, OFT and RV morphology is normal. In $Fgf8^{flox/flox}$ (D through F), $Fgf8^{flox/flox};Fgf10^{+/-}$ (G through I), and $Fgf8^{flox/flox};Fgf10^{-/-}$ (J through L) embryos, the angle between the proximal and distal regions of the OFT is more obtuse (lines) or, in severe cases, absent, and/or the RV is smaller (circle) when compared with normal hearts (A through C). M through O, Sections of the OFT of E10.5 embryos with the genotypes indicated. CNC has invaded the OFT (arrowheads), and the endothelium is beginning to undergo epithelial–mesenchymal transformation[31] (arrows), where the cushions will form in *Fgf8;Fgf10* double heterozygous control embryos (M). In *Fgf8;Fgf10* mutant embryos, these processes are compromised (N and O) and most notably in the double homozygous mutant, the OFT is smaller and misshapen (O). Pharyngeal arches are numbered in A. Scale bar=200 μm.

and ectoderm) of compound mutant embryos (Figure 2B). We could not detect differences between $Fgf8^{flox/+};Fgf10^{+/-}$ and $Fgf8^{flox/flox};Fgf10^{+/-}$ mutants, suggesting that FGF8 in pharyngeal endoderm and ectoderm, together with FGF10 from 1 allele of *Fgf10* expressed in mesoderm, lead to levels of *Pea3* and *Erm* transcription in the pharyngeal region that obscure the reduction in the mesoderm. However, significant downregulation of the signaling read out from all FGF sources was detected in *Fgf8;Fgf10* double homozygous mutants (Figure 2B). These results demonstrate the effect on FGF signaling readout of removing both alleles of *Fgf10* on an *Fgf8* mesodermal–null background. Transcripts for *Isl1*, a key transcription factor required in the SHF,[29] were also downregulated in the double homozygous mutants (Figure 2B). Apoptosis and proliferation were altered in Isl1-positive SHF cells in the double homozygous mutants (Online Figure I, A through D), as reported for $Fgf8^{flox/-}$ mutants,[19] thus explaining the reduction in *Isl1* transcripts.

Mesodermal FGF8 and FGF10 Regulate Development of the PAAs

PAAs, visualized by ink injection, were examined in *Fgf8;Fgf10* compound mutants at E10.5 (Figure 3). At this stage, normal mouse embryos have third, fourth, and sixth bilateral PAAs (Figure 3A through 3C). PAA development was affected in some $Fgf8^{flox/flox}$ embryos (Figure 3D through 3F and 3M). Ectodermal *Fgf8* ablation causes bilateral fourth PAA hypoplasia or aplasia.[25] With mesodermal deletion of *Fgf8*, we observed not only fourth PAA defects but also effects on the development of the third and sixth PAAs and abnormal maintenance of the second PAA (Figure 3M). $Fgf10^{-/-}$ mutants did not show any PAA defects, as reported previously (data not shown).[30] However, deletion of one allele of *Fgf10* increased the proportion of PAA defects in $Fgf8^{flox/flox}$ embryos (Figure 3G through 3I and 3M), and this incidence was further increased in *Fgf8;Fgf10* double homozygous mutants (Figure 3J through 3M). Apoptosis in CNC was observed at the level of the developing fourth PAA,

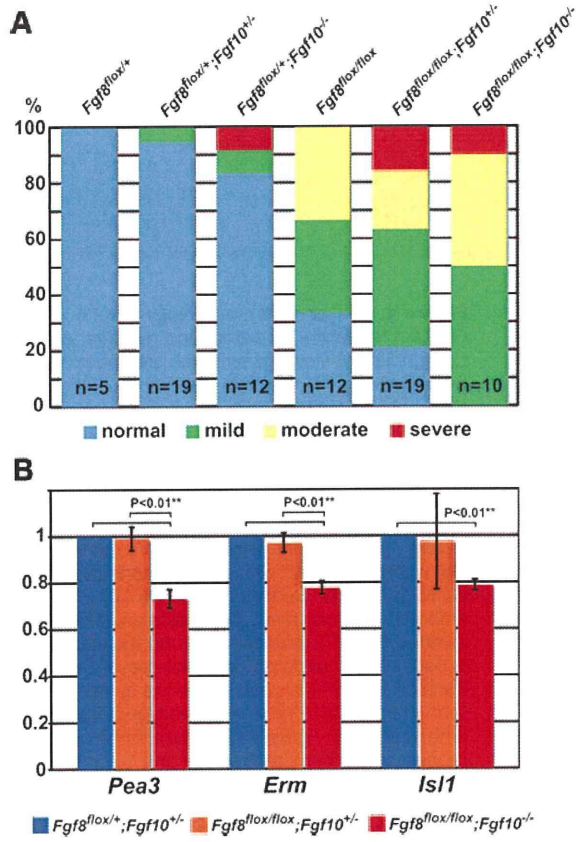

Figure 2. Reduction of FGF dosage affects morphology and gene expression in the OFT and RV. A, Phenotype of OFT and RV morphology of E9.5 *Fgf8*;*Fgf10*;*MesP1Cre* compound mutants are divided into normal, mild, moderate, and severe according to OFT length, the angle between the proximal and distal regions of the OFT, RV size, and looping, based on blind tests. Increasingly severe phenotypes (see Figure 1) are observed as *Fgf* gene dosage is reduced. Numbers of embryos (n) are indicated below each column. B, Quantitative PCR analysis of transcripts for FGF signaling effectors, *Pea3* and *Erm*, and for Isl1, normalized to *Gapdh* transcripts, in extracts from the pharyngeal region dissected from 6 embryos, with the genotypes indicated, at 24 to 26 somite stages. Results are shown relative to that for *Fgf8*;*Fgf10* double heterozygotes. Error bar indicates the SD.

in $Fgf8^{flox/flox}$;$Fgf10^{+/-}$ mutants (Online Figure I, E and F), as reported for *Fgf8* hypomorphic, $Fgf8^{flox/-}$;*AP2aIresCre*, and $Fgf8^{flox/-}$;*Hoxa3Cre* mutants.[23,25] Sections also illustrated the severe PAA defects seen in *Fgf8*;*Fgf10* double homozygous mutants (Figure 3O), compared to control *Fgf8*;*Fgf10* double heterozygous embryos (Figure 3N). These results, summarized in Table 1, show that mesodermal FGF8 and FGF10 are critical for PAA development.

Heart and PAA Phenotypes at Later Developmental Stages Are Consistent With Those Observed Earlier

The adult configuration of the heart and great vessels is largely established by E15.5: the ventricles are separated by the ventricular septum; the OFT has given rise to myocardium at the base of the aorta and pulmonary trunk; and the third, fourth, and sixth PAAs have been remodeled into the common carotid and subclavian arteries and contributed to part of the aortic arch and ductus arteriosus (Figure 4A and 4B). In the heart of $Fgf8^{flox/flox}$ embryos, as previously reported,[19] transposition of the great arteries, double outlet right ventricle (DORV), and ventricular septal defects (VSDs) were observed, although in a minority of cases (Figure 4F and 4G; Table 2). In $Fgf8^{flox/flox}$;*Fgf10* compound mutants, these heart defects became more frequent as *Fgf10* dosage is reduced (Figure 4J, 4L, and 4M; Table 2). Defects in PAA derivatives reflect the PAA abnormalities seen in mutants at E10.5. We observed absence of the left common carotid artery (Figure 4E, 4H, and 4K), which was attributable to loss of the left third PAA; aberrant origin of the right subclavian artery (Figure 4F, 4I, and 4K), which is attributable to loss of the right fourth PAA; right aortic arch (Figure 4I), which is caused by loss of the left fourth PAA (the aortic arch is probably replaced by the right fourth PAA); and narrow aortic arch (Figure 4L), because of a hypoplastic left fourth PAA. Consistent with earlier defects of the heart and PAA, the incidence of these later defects in surviving embryos was significantly increased when *Fgf10* gene dosage was reduced, in conjunction with mesodermal deletion of *Fgf8* (Table 2). These results confirm the functional overlap of mesodermal FGF8 and FGF10 in the development of the arterial pole of the heart and PAA, seen at earlier stages.

Discussion

The phenotypic analysis that we present establishes a role for FGF10 as well as FGF8 in the formation of the arterial pole of the heart and demonstrates that this process is highly sensitive to FGF dosage. Furthermore, we show that the level of FGF8 and FGF10 signaling is not only critical for OFT development, but also for the PAAs and their derivatives. Unexpectedly, mesodermal, as well as ectodermal,[25] expression of *Fgf8* is important for the correct formation of these arteries and thus for cardiac function.

Most of the mutant embryos survive to late fetal stages, permitting analysis of the definitive morphology of the arterial pole. This is in contrast to previously reported observations on $Fgf8^{flox/-}$;$MesP1^{Cre/+}$ embryos of which 65% died by E10.5.[19] This difference probably reflects the mesodermal specificity of deletion of the floxed alleles, which in our case ($Fgf8^{flox/flox}$;$MesP1^{Cre/+}$) are entirely responsible for generating the mutant phenotype. At early stages, in *Fgf8* and in *Fgf8*;*Fgf10* mutants, we observe hypoplasia of both the OFT and RV, which also derives from SHF cells expressing *Fgf8*,[15,20] as well as *Fgf10*.[15] This reflects apoptosis and loss of proliferation of progenitor cells, observed when FGF signaling is abrogated, attributable either to mutation of mesodermal *Fgf8* and *Fgf10* (in this study)[19] or to interference with FGF signal reception in the SHF.[31,32] A reduction in SHF cells is also indicated by a decrease in *Isl1* expression, reported for the more severe $Fgf8^{flox/-}$;*MesP1Cre* phenotype[19] and notable in $Fgf8^{flox/flox}$;$Fgf10^{-/-}$ double mutants. As the OFT matures, leading to epithelial–mesenchymal transition, cushion formation is initiated and CNC migrates into the OFT. These processes are affected when FGF signaling in mesoderm is abrogated,[31,32] and the phenotypes again are striking in the $Fgf8^{flox/flox}$;$Fgf10^{-/-}$ double mutants. The effects of FGF signaling from the SHF on CNC are indirect, because the arterial pole of the heart develops normally when FGF signaling

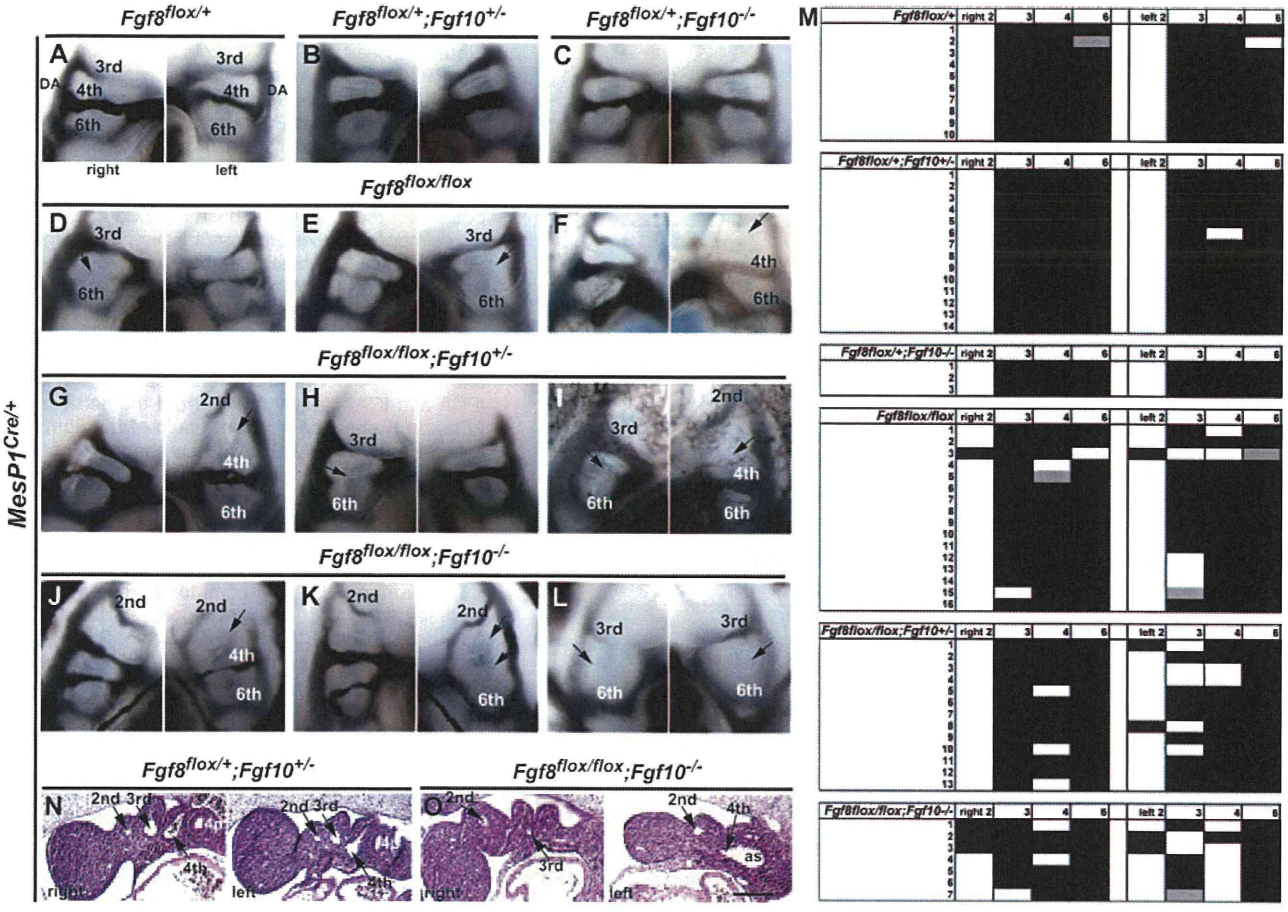

Figure 3. PAAs in *Fgf8*;*Fgf10*;*MesP1Cre* compound mutants. A through L, PAAs are visualized by ink injection at E10.5. Genotypes are listed above the images. At E10.5, third, fourth, and sixth PAAs are observed in the arches on both sides of the embryo. $Fgf8^{flox/+}$, $Fgf8^{flox/+}$;$Fgf10^{+/-}$, and $Fgf8^{flox/+}$;$Fgf10^{-/-}$ embryos have normal PAA patterns (A through C), whereas $Fgf8^{flox/flox}$, $Fgf8^{flox/flox}$;$Fgf10^{+/-}$ and $Fgf8^{flox/flox}$;$Fgf10^{-/-}$ embryos have various defects (arrows in D through L), including missing third, fourth, and sixth PAAs, and retention of the second PAA. M, Summary of ink injection results for each embryo examined. Black columns represent PAAs labeled by the ink; white columns, PAAs where ink labeling was negative; gray columns, PAAs that were weakly labeled. N and O, Sections of embryos at E10.0 in the region of the pharyngeal arches, with the genotypes indicated. In control *Fgf8*;*Fgf10* double heterozygous embryos, the second, third, and fourth arches are evident (N, arrows). The fourth pharyngeal pouch (4p) is also visible. In the *Fgf8*;*Fgf10* double homozygous mutant sections shown, the fourth arch is present but the PAA is not detectable on the right-hand side. On the left side, the third PAA is missing (O). as indicates aortic sac; DA, dorsal aorta. Scale bar=200 μm.

in CNC is diminished.[31,32] We propose that the Bmp/TGFβ pathway mediates the action of mesodermal FGF signaling on CNC, because components of this pathway are downregulated in *Fgf8* mutants.[31] This would also have effects on the Nkx2.5 transcriptional network in the SHF.[33] Further identification of targets of Pea3/Erm, transcriptional effectors of FGF signaling, should provide more insight into the FGF regulatory network. Failure of CNC migration into the OFT probably results from abnormal cell death in the pharyngeal arches.[20,23–25] Upregulation of FGF signaling, observed with CNC ablation[34] or in *Tbx3* mutants,[35] also disrupts OFT development, demonstrating a critical requirement for precise levels of FGF signaling during arterial pole formation. Because CNC contributes the smooth muscle of the nascent PAAs and their mature derivatives, CNC death in *Fgf8*; *Fgf10*;*MesP1Cre* compound mutants contributes to defects in the stabilization and remodeling of these arteries. In $Fgf8^{flox/-}$; *AP2αIresCre* mutants where *Fgf8* was deleted in pharyngeal ectoderm, major defects in the fourth PAA were documented, with minor effects on third and sixth PAAs.[25] *Fgf8* deletion in the mesodermal core of the arches causes similar effects on third, fourth and sixth PAAs. The increase in PAA defects in $Fgf8^{flox/flox}$; $Fgf10^{-/-}$ double mutants reveals an unsuspected role for FGF10 in PAA development. We also observe some cases of second PAA persistence at E10.5, probably reflecting a developmental delay. Mesodermal FGF signaling is clearly also necessary and the timing of this requirement may precede the appearance of CNC. *MesP1Cre* is activated at about E6.5, well before somites begin to form, whereas the *Mef2c* regulatory element that drives *Mef2cCre* expression in the SHF, including pharyngeal arch mesoderm, is activated later, from 2 to 3 somite stages.[19] Because PAA formation and remodeling are normal in $Fgf8^{flox/-}$; *Mef2cCre* embryos (16/16; A.M.M., unpublished data, 2005) the *MesP1Cre* phenotypes indicate that mesodermal FGF signaling is required at early stages to support PAA development, before CNC arrive in the arches.

Cardiac defects in surviving *Fgf8*;*Fgf10* mutants, present as alignment defects of the aorta and pulmonary trunk (transposition of the great arteries) together with DORV and

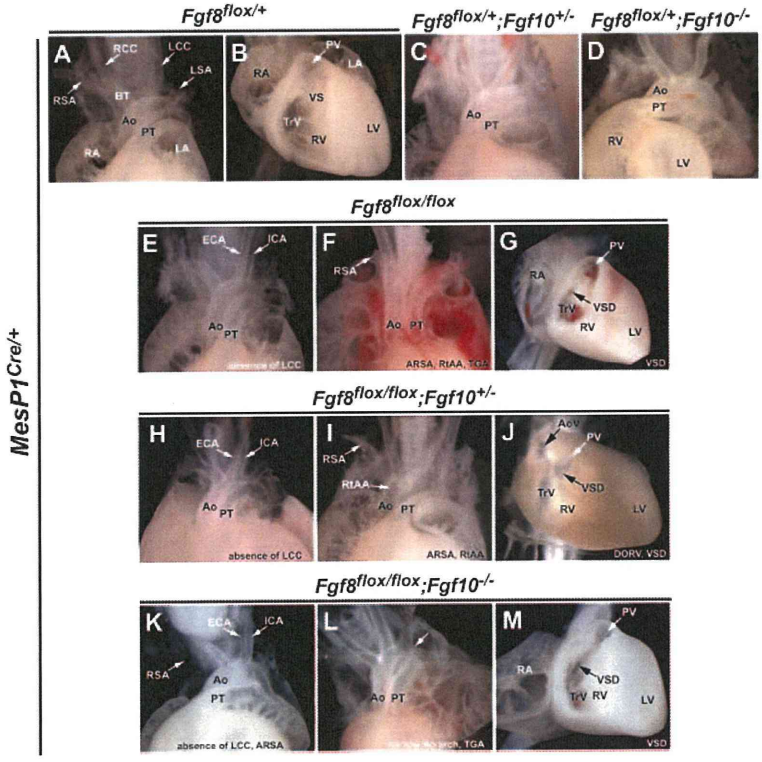

Figure 4. Heart and PAA defects in *Fgf8*;*Fgf10*; *MesP1Cre* compound mutants at later stages (E15.5 to E18.5). Genotypes are listed above the images. A through C, Heart and PAAs have normal structures in $Fgf8^{flox/+}$ and $Fgf8^{flox/+}$;$Fgf10^{+/-}$ embryos. In $Fgf8^{flox/+}Fgf10^{-/-}$ and $Fgf8^{flox/flox}$;$Fgf10^{-/-}$ embryos (D and K through M), in the absence of FGF10, the position of the apex of the heart is random, and the pulmonary arteries are absent; other parts of the $Fgf8^{flox/+}$;$Fgf10^{-/-}$ heart and the PAAs are normal (D). E through M, $Fgf8^{flox/flox}$ (E through G), $Fgf8^{flox/flox}$;$Fgf10^{+/-}$ (H through J), and $Fgf8^{flox/flox}$; $Fgf10^{-/-}$ (K through M) embryos have PAA and heart defects. As examples of PAA defects, E, H, and K show external and internal carotid arteries (ECA and ICA) directly arising from the aortic arch, F, I, and K show an aberrant origin of the right subclavian artery (ARSA), and an abnormal right aortic arch (RtAA) is also observed (I). Heart defects include abnormal alignment of the OFT (transposition of the great arteries [TGA]; DORV) (F, J, and L) and VSDs (G, J, and M). Ao indicates aorta; AoV, aortic valve; BT, brachiocephalic trunk; LA, left atrium; LCC, left common carotid artery; LSA, left subclavian artery; LV, left ventricle; PT, pulmonary trunk; PV, pulmonary valve; RA, right atrium; RCC, right common carotid artery; RSA, right subclavian artery; TrV, tricuspid valve; VS, ventricular septum.

VSDs, reflecting earlier malpositioning of the OFT and affected CNC. These defects also predominate when mesodermal *Fgf8* is mutated (Table 2), whereas persistent truncus arteriosus is seen when *Fgf8* is deleted in both mesoderm and pharyngeal endoderm.[13,19] The defects that we observe later in carotid and subclavian arteries and in the aortic arch reflect earlier defects in PAA development. When *Fgf8* is deleted in pharyngeal ectoderm,[25] the range and frequency of defects is different from those observed with mesodermal deletion of *Fgf8*, or when *Fgf10* is also mutated. In addition to dose dependence, this result reveals the importance of paracrine effects of FGF signaling during PAA development.

Deletion of *Fgf8* and *Fgf10* does not result in total loss of the structures that depend on FGF signaling. This may be because other signaling pathways, such as Bmp/TGFβ, which lies downstream of FGF8,[19] also function independently to promote formation of the arterial pole of the heart and the PAAs. It may also reflect the ability of other FGFs to compensate in the SHF and pharyngeal arches. *Fgf15*, for example, is expressed in pharyngeal mesoderm and *Fgf15* mutants have cardiac defects (DORV, overriding aorta and VSD), suggesting that FGF15 may play a role in the development of the arterial pole of the heart.[36] Loss of *Fgf3*, which is also expressed in pharyngeal endoderm, does not cause heart or PAA phenotypes, but $Fgf3^{-/-}$;$Tbx1^{+/-}$ mutants have an aberrant origin of the right subclavian artery and interrupted aortic arch.[37]

In considering the relative roles of FGF8 and FGF10, the former is more widely produced, by pharyngeal endoderm and pharyngeal ectoderm, as well as by mesoderm in the anterior SHF and in its extension into the core of the pharyngeal arches, whereas FGF10 production is predominantly limited to the mesoderm. Both FGFs bind to FGF receptor (FGFR)2, although FGF10 binds preferentially to the IIIb isoform, whereas FGF8 binds to IIIc and also has affinity for FGFR1, FGFR3IIIc, and FGFR4.[38–40] Mutational analysis of *Fgfr1* and *Fgfr2* suggests that FGFR1 is the dominant receptor in the SHF,[31] although FGFR2 is also active and indeed in a different genetic background may be more important.[32] Mutation of *Fgfr1* and *Fgfr2* in mesoderm compromises OFT development, as does overexpression of Sprouty2, an inhibitor of intracellular FGF signaling.[31] Examination of *Fgfr2-IIIb* mutants shows later cardiac defects,[16] but no striking effects on the early OFT, although RV hypoplasia, overriding aorta, DORV, and VSDs were noted. The question of in vivo FGF/receptor specificity is complex and the only clear conclusion to date is that FGFR1 and FGFR2 are required for FGF8 and FGF10 signaling, playing an essential role in the control of SHF progenitor cell proliferation and downstream signaling cascades[31] during OFT morphogenesis.

The *Tbx1* mutant phenotype, which recapitulates cardiovascular aspects of human DiGeorge syndrome,[41–43] overlaps with that of *Fgf8* hypomorphs.[23,24] *Tbx1* is expressed in the mesoderm of the anterior SHF, including the mesodermal core, endoderm, and ectoderm of the pharyngeal arches,[44,45] like *Fgf8*. Genetic analysis suggests that *Tbx1* lies upstream of *Fgf8* in pharyngeal endoderm[46] and also affects *Fgf8* and *Fgf10* expression in SHF mesoderm.[18,46,47] Phenotypic analysis of embryos after tissue specific deletion of *Tbx1* with mesodermal *Cre* lines has shown that mesodermal Tbx1 is critical for SHF and OFT development.[48] This is similar to FGF8[19] and to FGF10 as we now show.

Our findings demonstrate for the first time that mesodermal FGF10, as well as FGF8, is important for formation of the arterial pole of the heart and the PAAs, providing new insight into the cardiovascular abnormalities seen in Di-

George syndrome. Furthermore, mutations in *Fgf10* and *Fgf8* that affect their expression in pharyngeal mesoderm may underlie human congenital heart and vascular defects.

Acknowledgments

We thank Y. Saga for the $MesP1^{Cre/+}$ line and N. Itoh and S. Kato for $Fgf10^{+/-}$ mice. We thank C. Bodin and C. Cimper for help with histology, E. Pecnard and S. Coqueran for genotyping, E.J. Park for scoring of OFT/RV morphology of embryos, and to members of our laboratory and S. Zaffran for helpful discussions.

Sources of Funding

The work performed in the laboratory of M.E.B. was supported by the Institut Pasteur and the Centre National de la Recherche Scientifique, with grants from the European Union Integrated Project "Heart Repair" LHSM-CT2005-018630 (also to R.G.K.) and the CardioCell LT2009-223372 project. The work performed in the laboratory of A.M.M. was supported by the National Institute of Child Health and Development. Y.W. received a fellowship from the European Union Integrated Project "Heart Repair." S.M.-T. received a fellowship from the Naito Foundation to perform work for 6 months in the laboratory of M.E.B.

Disclosures

None.

References

1. Lloyd-Jones D, Adams R, Carnethon M, De Simone G, Ferguson TB, Flegal K, Ford E, Furie K, Go A, Greenlund K, Haase N, Hailpern S, Ho M, Howard V, Kissela B, Kittner S, Lackland D, Lisabeth L, Marelli A, McDermott M, Meigs J, Mozaffarian D, Nichol G, O'Donnell C, Roger V, Rosamond W, Sacco R, Sorlie P, Stafford R, Steinberger J, Thom T, Wasserthiel-Smoller S, Wong N, Wylie-Rosett J, Hong Y. Heart disease and stroke statistics–2009 update: a report from the American Heart Association Statistics Committee and Stroke Statistics Subcommittee. *Circulation*. 2009;119:e21–e181.
2. Nakajima Y, Yamagishi T, Hokari S, Nakamura H. Mechanisms involved in valvuloseptal endocardial cushion formation in early cardiogenesis: roles of transforming growth factor (TGF)-beta and bone morphogenetic protein (BMP). *Anat Rec*. 2000;258:119–127.
3. Webb S, Qayyum SR, Anderson RH, Lamers WH, Richardson MK. Septation and separation within the outflow tract of the developing heart. *J Anat*. 2003;202:327–342.
4. Buckingham M, Meilhac S, Zaffran S. Building the mammalian heart from two sources of myocardial cells. *Nat Rev Genet*. 2005;6:826–835.
5. Franco D, Meilhac SM, Christoffels VM, Kispert A, Buckingham M, Kelly RG. Left and right ventricular contributions to the formation of the interventricular septum in the mouse heart. *Dev Biol*. 2006;294:366–375.
6. Verzi MP, McCulley DJ, De Val S, Dodou E, Black BL. The right ventricle, outflow tract, and ventricular septum comprise a restricted expression domain within the secondary/anterior heart field. *Dev Biol*. 2005;287:134–145.
7. Waldo KL, Hutson MR, Ward CC, Zdanowicz M, Stadt HA, Kumiski D, Abu-Issa R, Kirby ML. Secondary heart field contributes myocardium and smooth muscle to the arterial pole of the developing heart. *Dev Biol*. 2005;281:78–90.
8. Jiang X, Rowitch DH, Soriano P, McMahon AP, Sucov HM. Fate of the mammalian cardiac neural crest. *Development*. 2000;127:1607–1616.
9. Nakamura T, Colbert MC, Robbins J. Neural crest cells retain multipotential characteristics in the developing valves and label the cardiac conduction system. *Circ Res*. 2006;98:1547–1554.
10. Hutson MR, Kirby ML. Model systems for the study of heart development and disease. Cardiac neural crest and conotruncal malformations. *Semin Cell Dev Biol*. 2007;18:101–110.
11. Waldo KL, Hutson MR, Stadt HA, Zdanowicz M, Zdanowicz J, Kirby ML. Cardiac neural crest is necessary for normal addition of the myocardium to the arterial pole from the secondary heart field. *Dev Biol*. 2005;281:66–77.
12. Rochais F, Mesbah K, Kelly RG. Signaling pathways controlling second heart field development. *Circ Res*. 2009;104:933–942.
13. Brown CB, Wenning JM, Lu MM, Epstein DJ, Meyers EN, Epstein JA. Cre-mediated excision of Fgf8 in the Tbx1 expression domain reveals a critical role for Fgf8 in cardiovascular development in the mouse. *Dev Biol*. 2004;267:190–202.
14. Engleka KA, Gitler AD, Zhang M, Zhou DD, High FA, Epstein JA. Insertion of Cre into the Pax3 locus creates a new allele of Splotch and identifies unexpected Pax3 derivatives. *Dev Biol*. 2005;280:396–406.
15. Kelly RG, Brown NA, Buckingham ME. The arterial pole of the mouse heart forms from Fgf10-expressing cells in pharyngeal mesoderm. *Dev Cell*. 2001;1:435–440.
16. Marguerie A, Bajolle F, Zaffran S, Brown NA, Dickson C, Buckingham ME, Kelly RG. Congenital heart defects in Fgfr2-IIIb and Fgf10 mutant mice. *Cardiovasc Res*. 2006;71:50–60.
17. Ryckebusch L, Wang Z, Bertrand N, Lin SC, Chi X, Schwartz R, Zaffran S, Niederreither K. Retinoic acid deficiency alters second heart field formation. *Proc Natl Acad Sci U S A*. 2008;105:2913–2918.
18. Hu T, Yamagishi H, Maeda J, McAnally J, Yamagishi C, Srivastava D. Tbx1 regulates fibroblast growth factors in the anterior heart field through a reinforcing autoregulatory loop involving forkhead transcription factors. *Development*. 2004;131:5491–5502.
19. Park EJ, Ogden LA, Talbot A, Evans S, Cai CL, Black BL, Frank DU, Moon AM. Required, tissue-specific roles for Fgf8 in outflow tract formation and remodeling. *Development*. 2006;133:2419–2433.
20. Ilagan R, Abu-Issa R, Brown D, Yang YP, Jiao K, Schwartz RJ, Klingensmith J, Meyers EN. Fgf8 is required for anterior heart field development. *Development*. 2006;133:2435–2445.
21. Crossley PH, Martin GR. The mouse Fgf8 gene encodes a family of polypeptides and is expressed in regions that direct outgrowth and patterning in the developing embryo. *Development*. 1995;121:439–451.
22. Sun X, Meyers EN, Lewandoski M, Martin GR. Targeted disruption of Fgf8 causes failure of cell migration in the gastrulating mouse embryo. *Genes Dev*. 1999;13:1834–1846.
23. Frank DU, Fotheringham LK, Brewer JA, Muglia LJ, Tristani-Firouzi M, Capecchi MR, Moon AM. An Fgf8 mouse mutant phenocopies human 22q11 deletion syndrome. *Development*. 2002;129:4591–4603.
24. Abu-Issa R, Smyth G, Smoak I, Yamamura K, Meyers EN. Fgf8 is required for pharyngeal arch and cardiovascular development in the mouse. *Development*. 2002;129:4613–4625.
25. Macatee TL, Hammond BP, Arenkiel BR, Francis L, Frank DU, Moon AM. Ablation of specific expression domains reveals discrete functions of ectoderm- and endoderm-derived FGF8 during cardiovascular and pharyngeal development. *Development*. 2003;130:6361–6374.
26. Sekine K, Ohuchi H, Fujiwara M, Yamasaki M, Yoshizawa T, Sato T, Yagishita N, Matsui D, Koga Y, Itoh N, Kato S. Fgf10 is essential for limb and lung formation. *Nat Genet*. 1999;21:138–141.
27. Saga Y, Miyagawa-Tomita S, Takagi A, Kitajima S, Miyazaki J, Inoue T. MesP1 is expressed in the heart precursor cells and required for the formation of a single heart tube. *Development*. 1999;126:3437–3447.
28. Liao J, Aggarwal VS, Nowotschin S, Bondarev A, Lipner S, Morrow BE. Identification of downstream genetic pathways of Tbx1 in the second heart field. *Dev Biol*. 2008;316:524–537.
29. Cai CL, Liang X, Shi Y, Chu PH, Pfaff SL, Chen J, Evans S. Isl1 identifies a cardiac progenitor population that proliferates prior to differentiation and contributes a majority of cells to the heart. *Dev Cell*. 2003;5:877–889.
30. Kelly RG, Papaioannou VE. Visualization of outflow tract development in the absence of Tbx1 using an FgF10 enhancer trap transgene. *Dev Dyn*. 2007;236:821–828.
31. Park EJ, Watanabe Y, Smyth G, Miyagawa-Tomita S, Meyers E, Klingensmith J, Camenisch T, Buckingham M, Moon AM. An FGF autocrine loop initiated in second heart field mesoderm regulates morphogenesis at the arterial pole of the heart. *Development*. 2008;135:3599–3610.
32. Zhang J, Lin Y, Zhang Y, Lan Y, Lin C, Moon AM, Schwartz RJ, Martin JF, Wang F. Frs2alpha-deficiency in cardiac progenitors disrupts a subset of FGF signals required for outflow tract morphogenesis. *Development*. 2008;135:3611–3622.
33. Prall OW, Menon MK, Solloway MJ, Watanabe Y, Zaffran S, Bajolle F, Biben C, McBride JJ, Robertson BR, Chaulet H, Stennard FA, Wise N, Schaft D, Wolstein O, Furtado MB, Shiratori H, Chien KR, Hamada H, Black BL, Saga Y, Robertson EJ, Buckingham ME, Harvey RP. An Nkx2–5/Bmp2/Smad1 negative feedback loop controls heart progenitor specification and proliferation. *Cell*. 2007;128:947–959.
34. Hutson MR, Zhang P, Stadt HA, Sato AK, Li YX, Burch J, Creazzo TL, Kirby ML. Cardiac arterial pole alignment is sensitive to FGF8 signaling in the pharynx. *Dev Biol*. 2006;295:486–497.

35. Mesbah K, Harrelson Z, Theveniau-Ruissy M, Papaioannou VE, Kelly RG. Tbx3 is required for outflow tract development. *Circ Res.* 2008;103: 743–750.
36. Vincentz JW, McWhirter JR, Murre C, Baldini A, Furuta Y. Fgf15 is required for proper morphogenesis of the mouse cardiac outflow tract. *Genesis.* 2005;41:192–201.
37. Aggarwal VS, Liao J, Bondarev A, Schimmang T, Lewandoski M, Locker J, Shanske A, Campione M, Morrow BE. Dissection of Tbx1 and Fgf interactions in mouse models of 22q11DS suggests functional redundancy. *Hum Mol Genet.* 2006;15:3219–3228.
38. Ornitz DM, Xu J, Colvin JS, McEwen DG, MacArthur CA, Coulier F, Gao G, Goldfarb M. Receptor specificity of the fibroblast growth factor family. *J Biol Chem.* 1996;271:15292–15297.
39. Powers CJ, McLeskey SW, Wellstein A. Fibroblast growth factors, their receptors and signaling. *Endocr Relat Cancer.* 2000;7:165–197.
40. Ohuchi H, Hori Y, Yamasaki M, Harada H, Sekine K, Kato S, Itoh N. FGF10 acts as a major ligand for FGF receptor 2 IIIb in mouse multi-organ development. *Biochem Biophys Res Commun.* 2000;277:643–649.
41. Jerome LA, Papaioannou VE. DiGeorge syndrome phenotype in mice mutant for the T-box gene, Tbx1. *Nat Genet.* 2001;27:286–291.
42. Lindsay EA, Vitelli F, Su H, Morishima M, Huynh T, Pramparo T, Jurecic V, Ogunrinu G, Sutherland HF, Scambler PJ, Bradley A, Baldini A. Tbx1 haploinsufficieny in the DiGeorge syndrome region causes aortic arch defects in mice. *Nature.* 2001;410:97–101.
43. Merscher S, Funke B, Epstein JA, Heyer J, Puech A, Lu MM, Xavier RJ, Demay MB, Russell RG, Factor S, Tokooya K, Jore BS, Lopez M, Pandita RK, Lia M, Carrion D, Xu H, Schorle H, Kobler JB, Scambler P, Wynshaw-Boris A, Skoultchi AI, Morrow BE, Kucherlapati R. TBX1 is responsible for cardiovascular defects in velo-cardio-facial/DiGeorge syndrome. *Cell.* 2001;104:619–629.
44. Garg V, Yamagishi C, Hu T, Kathiriya IS, Yamagishi H, Srivastava D. Tbx1, a DiGeorge syndrome candidate gene, is regulated by sonic hedgehog during pharyngeal arch development. *Dev Biol.* 2001;235: 62–73.
45. Vitelli F, Morishima M, Taddei I, Lindsay EA, Baldini A. Tbx1 mutation causes multiple cardiovascular defects and disrupts neural crest and cranial nerve migratory pathways. *Hum Mol Genet.* 2002;11:915–922.
46. Zhang Z, Cerrato F, Xu H, Vitelli F, Morishima M, Vincentz J, Furuta Y, Ma L, Martin JF, Baldini A, Lindsay E. Tbx1 expression in pharyngeal epithelia is necessary for pharyngeal arch artery development. *Development.* 2005; 132:5307–5315.
47. Vitelli F, Taddei I, Morishima M, Meyers EN, Lindsay EA, Baldini A. A genetic link between Tbx1 and fibroblast growth factor signaling. *Development.* 2002;129:4605–4611.
48. Zhang Z, Huynh T, Baldini A. Mesodermal expression of Tbx1 is necessary and sufficient for pharyngeal arch and cardiac outflow tract development. *Development.* 2006;133:3587–3595.

Novelty and Significance

What Is Known?

- FGF8 signaling from pharyngeal ectoderm is required for correct formation of great arteries.
- FGF8 from second heart field mesoderm is required for arterial pole formation.
- *Fgf10*, like *Fgf8*, is expressed in mesodermal cells of the second heart field.
- *Fgf10* mutants have no detectable great artery or arterial pole defects.

What New Information Does This Article Contribute?

- It reveals a new role of FGF10 in formation of the arterial pole of the heart, when FGF8 is reduced or abolished.
- It reveals a previously unexpected role for mesodermal FGF8 function in great vessel development.

More than 30% of congenital heart defects affect development of the arterial pole of the heart. In the mammalian embryo, cells that will contribute to this part of the heart derive from mesoderm of the second heart field. Loss of *Fgf8* function in these cells leads to arterial pole defects. *Fgf10* is also expressed in the second heart field, yet *Fgf10* mutants do not have detectable outflow tract or great vessel defects. This may be attributable to compensation by fibroblast growth factor (FGF)8. To address this question, we examined compound mutants and show that arterial pole defects are more severe in the absence of both *Fgf8* and *Fgf10* function in the second heart field. This is also the case for arch arteries that contribute connecting vessels, such as the subclavian and common carotid arteries, revealing for the first time a role for mesodermal FGF8 and FGF10 in vascular development. Our compound mutant analysis also demonstrates that this requirement is highly dosage sensitive, such that progressive reduction in the number of functional alleles of *Fgf8* and *Fgf10* leads to increasingly severe defects. These findings identify *Fgf8* and *Fgf10* as candidate genes for congenital cardiovascular malformations in the human population.

Supplement Material

Online Method

TUNEL assay and Immunohistochemstry

An In Situ Cell Death Detection Kit (Roche) was used for the TUNEL assay. Phospho-Histone H3 antibody (Cell Signaling Technology #9701), Isl1 (DSHB #39.4D5) and AP2α (DSHB #3B5) antibodies were used for immunohistochemistry.

Online Table I. Number of embryos obtained from *Fgf8$^{flox/+}$;Fgf10$^{+/-}$;MesP1$^{Cre/+}$* x *Fgf8$^{flox/flox}$;Fgf10$^{+/-}$* crosses.

Genotype *Fgf8;Fgf10;Cre*	E9.5	E10.5	E15.5/16.5	E18.5	Expected
flox/+;+/+	6 (3.64%)	4 (3.64%)	4 (5.56%)	4 (7.14%)	6.25%
flox/+;+/-	28 (16.97%)	12 (10.91%)	7 (9.72%)	6 (10.71%)	12.5%
flox/+;-/-	9 (5.45%)	2 (1.82%)	2 (2.78%)	2 (3.57%)	6.25%
flox/flox;+/+	11 (6.67%)	12 (10.91%)	5 (6.94%)	7 (12.5%)	6.25%
flox/flox;+/-	18 (10.91%)	15 (13.64%)	7 (9.72%)	6 (10.71%)	12.5%
flox/flox;-/-	14 (8.48%)	10 (9.09%)	3 (4.17%)	2 (3.57%)	6.25%
Total number	165	110	72	56	

Online Figure legend

Online Figure I. Apoptosis and proliferation in *Fgf8;Fgf10* compound mutants. (A-F) TUNEL assay was performed at E9.5. (A,C) Control *Fgf8$^{flox/+}$;Fgf10$^{+/-}$* embryo shows some cell death in the pharyngeal endoderm (PE) (arrow heads). (B,D) This is increased in the PE and OFT of the *Fgf8$^{flox/flox}$;Fgf10$^{-/-}$* mutant. (A,B) The number of phospho-histone H3 (PHH3) positive cells (arrows) is also less in *Fgf8$^{flox/flox}$;Fgf10$^{-/-}$* mutants (B) compared to control *Fgf8$^{flox/+}$;Fgf10$^{+/-}$* embryos (A). (E,F) Transverse sections at the level of developing fourth PAA in E9.5 embryos show apoptosis in the AP2α-positive cells on the right side of the *Fgf8$^{flox/flox}$;Fgf10$^{+/-}$* mutant (E), but not in control *Fgf8$^{flox/+}$;Fgf10$^{+/-}$* embryos (F). Asterisks indicate the dorsal aorta.

Online Figure I

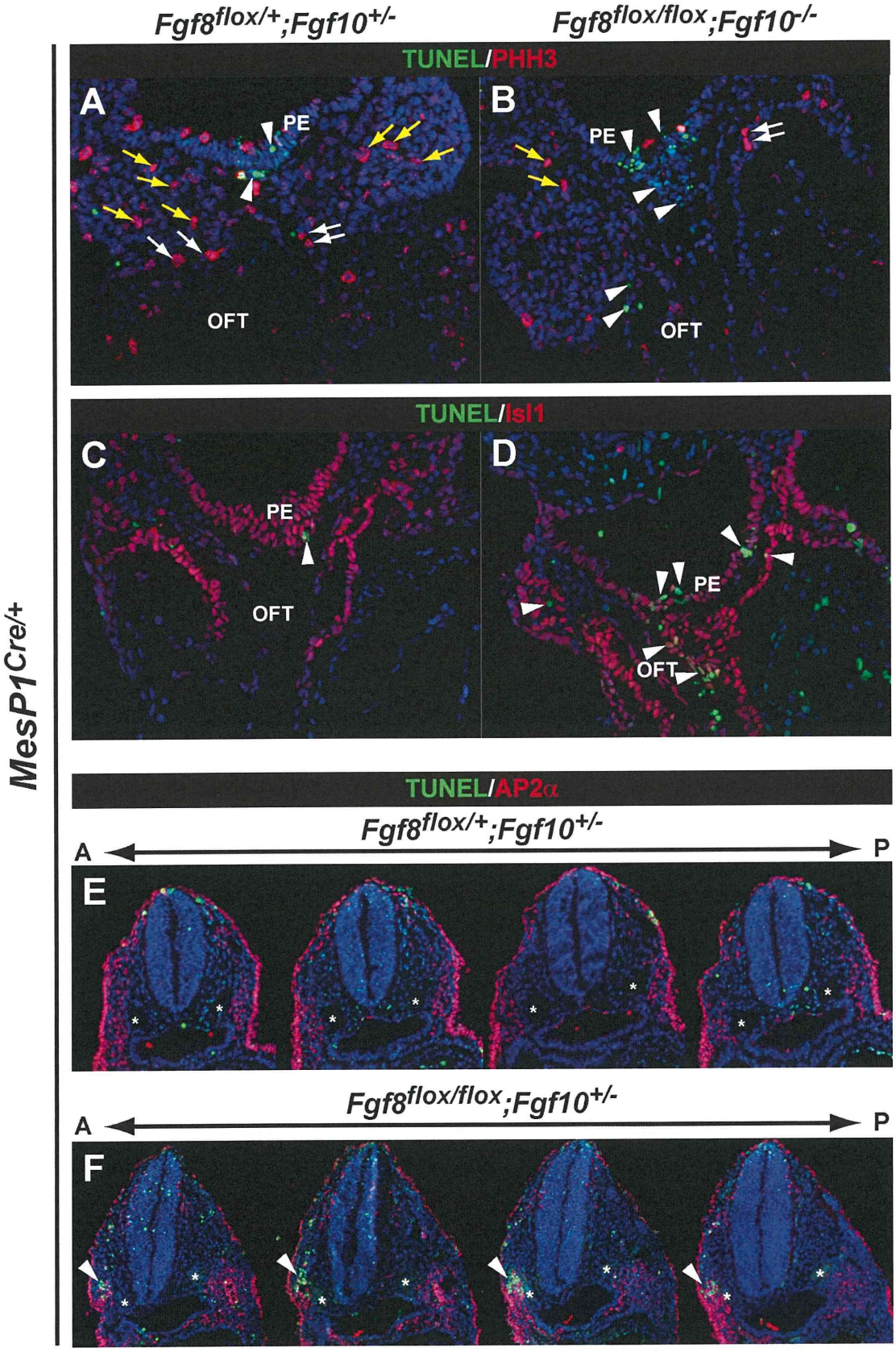

THE JOURNAL OF BIOLOGICAL CHEMISTRY VOL. 285, NO. 43, pp. 33018–33027, October 22, 2010

Pin1 Associates with and Induces Translocation of CRTC2 to the Cytosol, Thereby Suppressing cAMP-responsive Element Transcriptional Activity*[S]

Received for publication, April 26, 2010, and in revised form, July 9, 2010 Published, JBC Papers in Press, July 30, 2010, DOI 10.1074/jbc.M110.137836

Yusuke Nakatsu,[a1] Hideyuki Sakoda,[b1] Akifumi Kushiyama,[c] Hiraku Ono,[b] Midori Fujishiro,[b] Nanao Horike,[d] Masayasu Yoneda,[a] Haruya Ohno,[a] Yoshihiro Tsuchiya,[a] Hideaki Kamata,[a] Hidetoshi Tahara,[e] Toshiaki Isobe,[f] Fusanori Nishimura,[g] Hideki Katagiri,[h] Yoshitomo Oka,[h] Toshiaki Fukushima,[a] Shin-Ichiro Takahashi,[i] Hiroki Kurihara,[d] Takafumi Uchida,[j] and Tomoichiro Asano[a2]

From the [a]Department of Medical Science, Graduate School of Medicine, University of Hiroshima, 1-2-3 Kasumi, Minami-ku, Hiroshima City, Hiroshima 734-8553, Japan, the Departments of [b]Internal Medicine and [d]Physiological Chemistry and Metabolism, Graduate School of Medicine, and the [i]Department of Applied Biological Chemistry, Graduate School of Agricultural and Life Sciences, University of Tokyo, 7-3-1 Hongo, Bunkyo-ku, Tokyo 113-0033, Japan, the [c]Institute for Adult Disease, Asahi Life Foundation, Tokyo 100-0006, Japan, the [e]Department of Cellular and Molecular Biology, Graduate School of Biomedical Sciences, Hiroshima University, Hiroshima 734-8553, Japan, the [f]Center for Priority Areas, Tokyo Metropolitan University, Hachioji, Tokyo 192-0397, Japan, the [g]Department of Dental Science for Health Promotion, Hiroshima University Graduate School of Biomedical Sciences, Hiroshima 734-8553, Japan, the [h]Division of Molecular Metabolism and Diabetes, Tohoku University Graduate School of Medicine, 2-1 Seiryo-machi, Aoba-ku, Sendai 980-8575, Japan, and the [j]Department of Molecular Cell Biology, Graduate School of Agricultural Science, Tohoku University, Sendai, Miyagi 981-8555, Japan

Pin1 is a unique regulator, which catalyzes the conversion of a specific phospho-Ser/Thr-Pro-containing motif in target proteins. Herein, we identified CRTC2 as a Pin1-binding protein by overexpressing Pin1 with Myc and FLAG tags in mouse livers and subsequent purification of the complex containing Pin1. The association between Pin1 and CRTC2 was observed not only in overexpression experiments but also endogenously in the mouse liver. Interestingly, Ser^{136} in the nuclear localization signal of CRTC2 was shown to be involved in the association with Pin1. Pin1 overexpression in HepG2 cells attenuated forskolin-induced nuclear localization of CRTC2 and cAMP-responsive element (CRE) transcriptional activity, whereas gene knockdown of Pin1 by siRNA enhanced both. Pin1 also associated with CRTC1, leading to their cytosol localization, essentially similar to the action of CRTC2. Furthermore, it was shown that CRTC2 associated with Pin1 did not bind to CREB. Taken together, these observations indicate the association of Pin1 with CRTC2 to decrease the nuclear CBP·CRTC·CREB complex. Indeed, adenoviral gene transfer of Pin1 into diabetic mice improved hyperglycemia in conjunction with normalizing phosphoenolpyruvate carboxykinase mRNA expression levels, which is regulated by CRE transcriptional activity. In conclusion, Pin1 regulates CRE transcriptional activity, by associating with CRTC1 or CRTC2.

Pin1 was initially cloned as a NIMA kinase-interacting protein (1). Since its discovery, numerous proteins have been identified as Pin1 substrates, including p53, cyclin D1, and Tau (2–5). Pin1 interacts with a number of target proteins through recognition of phospho-Ser/Pro motifs, and the proline conformational change induced by Pin1 modifies the structures and functions, such as stabilization, phosphorylation, and translocation, of target proteins (4–7). Pin1 possesses the WW and PPIase[3] domains in its N-terminal (amino acids 1–38) and C-terminal (amino acids 39–163) regions, respectively. To date, many reports have supported an important role for Pin1 in diseases such as cancer and Alzheimer disease (4, 5). In this study, we demonstrated that Pin1 is also involved in metabolic disease via regulation of CRTC2 (CREB-regulated transcriptional co-activator 2; also known as TORC).

The cAMP-responsive element (CRE)-binding protein (CREB) stimulates transcriptional activity through recruitment of the histone acetylase CBP and through an association with CRTC, leading to formation of the CREB·CBP·CTRC complex on a CRE site (8–16). Thus, multiple molecular mechanisms affect the CREB·CBP·CTRC complex, resulting in the regulation of CRE transcriptional activity. They include the phosphorylations of CREB at Ser^{133}, CBP at Ser^{436}, and CRTC2 at Ser^{171} (16, 17). The phosphorylation of CRTC2 at Ser^{171} reportedly leads to an association with 14-3-3 protein and thereby to its nuclear exclusion and degradation (16).

The CRTC family consists of three members, CRTC1, CRTC2, and CRTC3 (16, 18). CRTC1 is highly expressed in the brain, whereas the other two are ubiquitously expressed (19). In the liver, insulin induces the phosphorylation of CRTC2 at Ser^{171}, and this phosphorylation leads to the aforementioned

* This work was supported in part by Grant-in-aid for Young Scientists 20790648 (to Y. N.) from the Ministry of Education, Science, Sports, and Culture, Japan.

[S] The on-line version of this article (available at http://www.jbc.org) contains supplemental Figs. 1–8.

[1] These authors contributed equally to this work.

[2] To whom correspondence should be addressed. Tel.: 81-82-257-5135; Fax: 81-82-257-5136; E-mail: asano-tky@umin.ac.jp.

[3] The abbreviations used are: PPIase, peptidyl-prolyl *cis/trans*-isomerase; CRE, cAMP-response element; CREB, CRE-binding protein; NLS, nuclear localization signal; MEF, mouse embryo fibroblast; STZ, streptozotocin; PEPCK, phosphoenolpyruvate carboxykinase; CRTC, CREB-regulated transcriptional co-activator.

association with 14-3-3 protein and the nuclear exclusion and degradation of CRTC2 (16, 20). In contrast, glucagon induces dephosphorylation of CRTC2 and translocation from the cytosol to the nucleus, thereby forming the CREB·CBP·CRTC2 complex and inducing gluconeogenesis (21). Thus, CRTC2 plays important roles in hepatic glucose metabolism.

In this study, we identified CRTC2 as a Pin1-binding protein. Interestingly, the portion of CRTC2 responsible for the association with Pin1 was revealed to be in the nuclear localization signal (NLS) domain. Herein, we demonstrate that Pin1 regulates the functions and subcellular localizations of CRTC family proteins, thereby altering CRE transcriptional activity.

EXPERIMENTAL PROCEDURES

Materials—Anti-Pin1 antibody was generated by immunizing rabbits with the peptide QMQKPFEDASFATRTGEMSGPVFTDSGIHIITRTE (amino acids 129–163 of human Pin1). Anti-FLAG tag and Myc tag antibodies were purchased from Sigma-Aldrich. The antibodies against CRTC2, CREB, 14-3-3 protein, GFP, and DsRed were purchased from Cell Signaling Technology. Anti-rabbit HRP antibodies conjugated to horseradish peroxidase were obtained from Amersham Biosciences. Dulbecco's modified Eagle's medium (DMEM) and fetal bovine serum were purchased from Invitrogen. All other reagents were of analytical grade.

Preparation of Adenoviruses Expressing MEF-tagged Pin1, CRTC1, and CRTC2—The Myc-TEV-FLAG (MEF) tag cassette was generated by DNA synthesis and inserted into cloning sites in the mammalian expression vector pcDNA3 (Invitrogen; termed pcDNA3-MEF), as reported previously (22). To create the N-terminally MEF-tagged Pin1 construct, human Pin1 cDNA was inserted into pcDNA3-MEF. Then the coding portion of MEF-tagged Pin1 was isolated from pcDNA3-MEF-Pin1, and the recombinant adenoviruses containing the cDNA coding for MEF-tagged Pin1 were constructed as described previously (22). Recombinant adenoviruses expressing human Pin1 with the C-terminal HA tag or N-terminal MEF tag were also constructed and used for adenoviral gene transfer to HepG2 cells and mouse liver. Similarly, adenoviruses expressing GFP-tagged CTRC1, CRTC2, and GFP-tagged CRTC2 were prepared. Adenovirus encoding LacZ served as a control, and the adenoviral gene transfer was performed as reported previously (22).

Purification of MEF-tagged Pin1 from Mouse Livers—Recombinant adenovirus expressing MEF-tagged Pin1 was generated, purified, and concentrated using cesium chloride ultracentrifugation as reported previously (22). Adenovirus encoding LacZ served as a control. Male mice, 9 weeks of age, were obtained from the Nippon Bio-Supp. Center (Tokyo, Japan). They were injected, via the tail vein, with adenovirus at a dose of 2.5×10^7 plaque-forming units/g body weight. Four days after adenovirus injection, the mouse livers were removed and lysed in lysis buffer (50 mM Tris-HCl, pH 7.5, 150 mM NaCl, 10% (w/v) glycerol, 100 mM NaF, 10 mM EGTA, 1 mM Na_3VO_4, 1% (w/v) Triton X-100, 5 μM $ZnCl_2$, 2 mM phenylmethylsulfonyl fluoride, 10 μg/ml aprotinin, and 1 μg/ml leupeptin). The lysates were centrifuged at 100,000 $\times$ *g* for 20 min at 4 °C. The supernatant was passed through a 5-μm filter, incubated with 150 μl of Sepharose beads for 60 min at 4 °C and then passed through a 0.65-μm filter. The filtrated supernatant was mixed with 150 μl of anti-Myc-conjugated Sepharose beads for the first immunoprecipitation. After incubation for 90 min at 4 °C, the beads were washed five times with 1.5 ml of TNTG buffer (20 mM Tris-HCl, pH 7.5, 150 mM NaCl, 10% (w/v) glycerol, 0.1% (w/v) Triton X-100), twice with buffer A (20 mM Tris-HCl, pH 7.5, 150 mM NaCl, and 0.1% (w/v) Triton X-100), and finally once with TNT buffer (50 mM Tris-HCl, pH 8.0, 150 mM NaCl, 0.1% (w/v) Triton X-100). The washed beads were incubated with 15 units of TEV protease (Invitrogen) in 150 μl of TNT buffer to release bound materials from the beads. After incubation for 60 min at room temperature, the supernatant was pooled, and the beads were washed twice with 75 μl of buffer A. The resulting supernatants were combined and incubated with 25 μl of FLAG-Sepharose beads for the second immunoprecipitation. After incubation for 60 min at room temperature, the beads were washed three times with 500 μl of buffer A, and proteins bound to the FLAG beads were dissociated by incubation with 1 mM synthetic FLAG peptides in buffer A for 120 min at 4 °C. Approximately 3 μg of protein (0.01% of starting materials) were routinely recovered by this procedure. The samples were electrophoresed and subjected to SDS-PAGE and immunoblotting.

Cell Culture—Sf9 cells were grown in TC100 (Invitrogen) medium containing 10% fetal calf serum at 27 °C. HepG2 hepatoma cells were grown in DMEM containing 10% fetal calf serum at 37 °C in 5% (v/v) CO_2 in air.

Preparation of Baculoviruses Expressing Pin1 and CRTC2 Constructs—The full-length coding regions of human Pin1, GFP, GFP-tagged Pin1, CRTC2, and DsRed-tagged full-length and various deletion mutant forms of CRTC2 and S136A CRTC2 were subcloned into pBacPAK9 transfer vector (Clontech), and the baculoviruses were prepared according to the manufacturer's instructions. For protein production, Sf9 cells were infected with these baculoviruses and grown for 48 h.

Preparation of Glutathione S-Transferase (GST)-Pin1 Fusion Protein—The cDNAs encoding full-length human Pin1, the WW domain of Pin1, and the PPIase domain of Pin1 were subcloned into a pGEX-5X-1 vector (Amersham Biosciences), which was used to transform *Escherichia coli* JM105 (Promega). Transformed cells were grown to an A_{600} of 0.6 in LB medium supplemented with 0.1 mg/ml ampicillin and stimulated for 3 h with 1.0 mM isopropyl-β-D-thiogalactopyranoside. GST fusion proteins were conjugated to glutathione-Sepharose 4B (Amersham Biosciences) and used for GST pull-down experiments.

GST Pull-down—HepG2 cells expressing MEF-CTRC2 and its mutants were homogenized with homogenizing buffer (20 mmol/liter Tris/HCl (pH 7.4), 1% Triton X-100, 0.25% sodium deoxycholate, 0.25 mol/liter NaCl) containing 0.2 mmol/liter phenylmethylsulfonyl fluoride and 5 μg/ml aprotinin and centrifuged at 15,000 rpm for 30 min at 4 °C, and the supernatants were then recentrifuged at 100,000 $\times$ *g* for 1 h. The supernatants (2 μg/ml protein concentration) were incubated with 1 ml of glutathione-Sepharose 4B for 1 h at 4 °C to remove nonspecifically bound proteins and then incubated with purified GST alone, GST-Pin1, and GST-Pin1 deletion mutant proteins for 1 h and finally washed six times with homogenizing buffer. glutathione-Sepharose 4B beads

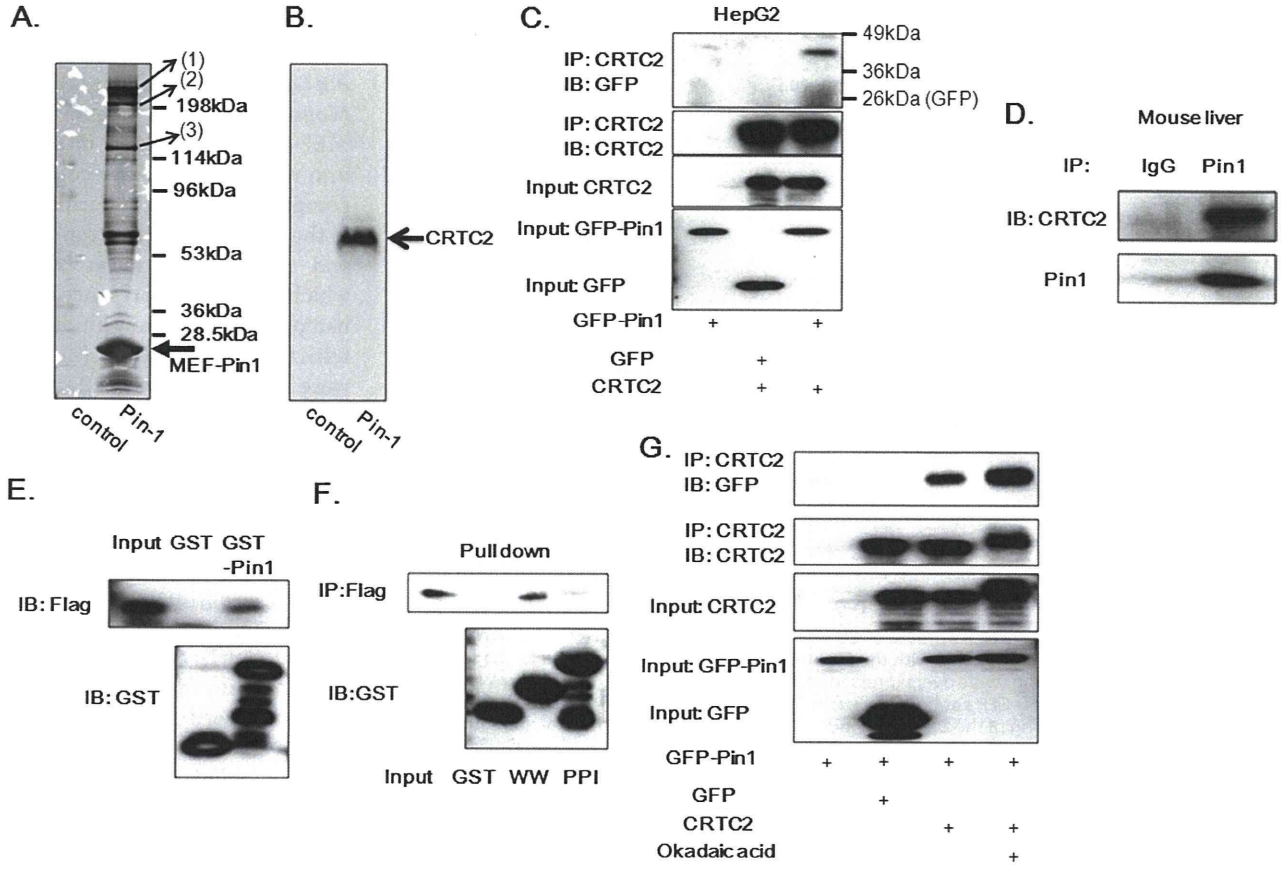

FIGURE 1. **Pin1 associates with CRTC2.** *A* and *B*, Pin1 with the N-terminal MEF tag was overexpressed in the mouse liver using adenovirus gene transfer, and the Pin1-containing complex was purified. The samples were electrophoresed and subjected to silver staining (*A*). Analysis using LC/MS revealed: *Band* (*1*), DNA-directed RNA polymerase II A; *Band* (*2*), suppressor of Ty 6 homolog + DNA-directed RNA polymerase II A; *Band* (*3*), DNA-directed RNA polymerase II polypeptide B + DNA-directed RNA polymerase I. *B*, the samples were subjected to the immunoblotting with anti-CRTC2 antibody. *C*, CRTC2 or control LacZ was overexpressed with GFP or GFP-Pin1. Then the cell lysates were immunoprecipitated (*IP*) with anti-CRTC2 antibody, followed by immunoblotting (*IB*) with anti-GFP antibody. *D*, the cell lysates from the mouse liver were immunoprecipitated with control IgG or anti-Pin1, and the immunoprecipitates were then immunoblotted with anti-CRTC2 and anti-Pin-1. *E*, HepG2 cell lysates expressing CRTC2 with a FLAG tag were incubated with glutathione beads conjugated with GST or GST-Pin1. After washing the beads, SDS-PAGE was performed followed by immunoblotting with anti-FLAG or anti-GST antibodies. *F*, HepG2 cell lysates expressing CRTC2 with a FLAG tag were incubated with glutathione beads conjugated with GST, the GST-WW domain, or the GST-PPI domain. After washing the beads, SDS-PAGE was performed, followed by immunoblotting with anti-FLAG or anti-GST antibodies. *G*, CRTC2 and either GFP or GFP-Pin1 were simultaneously overexpressed in HepG2 cells. With or without okadaic acid treatment for 0.5 h, the cell lysates were immunoprecipitated with anti-CRTC2, followed by immunoblotting with anti-GFP antibody. Representative immunoblotting data from three independent experiments are shown.

were boiled in Laemmli sample buffer, which was used for the SDS-PAGE and immunoblotting.

Preparation of Streptozotocin-treated Diabetic Mice and Gene Transfer of Pin1 into Mouse Livers—Streptozotocin (STZ)-treated diabetic male C57BL/6 mice (8–10 weeks of age) were prepared as reported previously (20). These mice were injected, via the tail vein, with adenovirus at a dose of 2.5×10^7 plaque-forming units/g body weight. Animals were fasted for 14 h and then were refed for 4 h before sacrifice. Blood glucose was measured with a portable blood glucose monitor, Glutest-Ace (Sanwa Kagaku Kenkyusho, Nagoya, Japan). All animal studies were conducted according to the Japanese guidelines for the care and use of experimental animals.

Immunoprecipitation and Immunoblotting—For the immunoprecipitation experiments, whole-cell extracts from HepG2 or Sf9 cells or mouse liver lysates obtained after an overnight fast were prepared in lysis buffer, as described above. Cell or tissue extracts were incubated for 4 h at 4 °C with the indicated antibody and then for 1 h with 30 μl of protein G-Sepharose beads. The pellets were washed five times with 1 ml of lysis buffer and then resuspended in Laemmli sample buffer, boiled for 3 min, and analyzed on SDS-polyacrylamide gels.

Western blot analysis was carried out as described previously (22). In brief, 10 μg of protein were separated by SDS-PAGE and electrophoretically transferred to polyvinylidene difluoride membranes in a transfer buffer consisting of 20 mM Tris-HCl, 150 mM glycine, and 20% methanol. The membranes were blocked with 5% nonfat dry milk in Tris-buffered saline with 0.1% Tween 20 and incubated with specific antibodies, followed by incubation with horseradish peroxidase-conjugated secondary antibodies. The antigen-antibody interactions were visualized by incubation with ECL chemiluminescence reagent (Amersham Biosciences).

Immunostaining—HepG2 cells were fixed with 4% paraformaldehyde for 10 min, rinsed with phosphate-buffered saline (PBS), and then exposed to 0.2% Triton X-100 in PBS for 5 min. Cells were subsequently incubated for 1 h at room temperature with anti-rabbit CRTC2 (1:500), and fluorescein isothiocya-

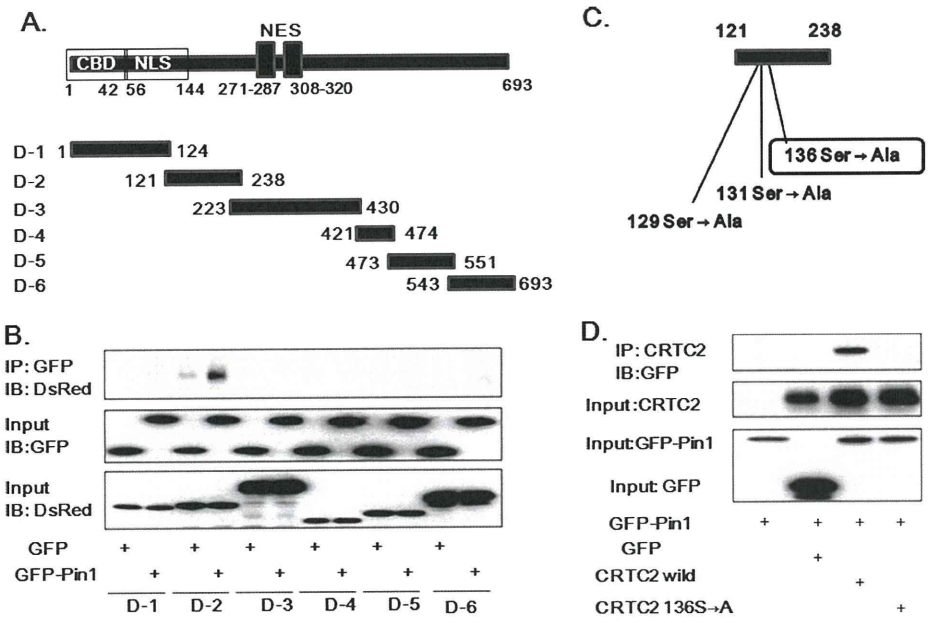

FIGURE 2. **Pin1 associates with the NLS domain of CRTC2.** *A*, the constructs of CRTC2 deletion mutants and baculoviruses expressing these six mutants with the C-terminal DsRed tag were prepared. *B*, the six deletion mutants with C-terminal DsRed tags were overexpressed with GFP or GFP-Pin1 in Sf9 cells. The cell lysates were immunoprecipitated (*IP*) with anti-GFP antibody, followed by immunoblotting (*IB*) with anti-DsRed antibody. The *upper panel* shows the binding of the Deletion-2 mutant to GFP-Pin1 but not to GFP alone. *C*, the orientations of three candidate Ser/Pro motifs in the Deletion-2 mutant involved in the association with Pin1. *D*, wild-type CRTC2 or CRTC2 S136A was overexpressed with GFP-Pin1 or GFP in Sf9 cells. The cell lysates were immunoprecipitated with anti-CRTC2 antibody followed by immunoblotting with anti-GFP. The *upper panel* shows that CRTC2 S136A does not associate with Pin1, unlike the wild-type CRTC2. Representative immunoblotting data from three independent experiments are shown.

nate-labeled anti-rabbit IgG (1:750) was used as the secondary antibody. Immunofluorescence was visualized with a laser-scanning confocal imaging system.

Luciferase Assay—The following plasmids were obtained from commercial sources: pTAL and pTAL-CRE from Clontech (Palo Alto, CA), pM from Stratagene (La Jolla, CA), and pGL4 and pRL-TK from Promega (Madison, WI). HepG2 cells in a 24-well collagen-coated plate were co-transfected with pTAL-CRE vector (0.25 μg/well) with an internal reporter, pRL-TK (0.25 μg). Luciferase activities were determined using the Dual-Luciferase Reporter Assay System (Promega Corp.).

RNA Analysis—RNA extractions were carried out using TRIzol, followed by purification over a QIAEASY RNA column. Reverse transcription and quantitative PCR were carried out as already described. The primer set for human phosphoenolpyruvate carboxykinase (PEPCK) was GGTTCCCAGGGTGCATGAAA and CACGTAGGGTGAATCCGTCAG (114 bp), and that for human GAPDH was ACCACAGTCCATGCCATCAC and TCCACCACCCTGTTGCTGTA (451 bp).

Chromatin Immunoprecipitation Assay with Anti-CRTC2, CBP, or CREB Antibodies—HepG2 cells with or without forskolin stimulation were immunoprecipitated with anti-CRTC2, anti-CBP, or anti-CREB antibody, using the Chip-IT™ express enzymatic kit (Active Motif Corp.). Then precipitated DNA was amplified by PCR using primers against the relevant promoters.

Statistical Analysis—Results are expressed as means ± S.E., and significance was assessed using one-way analysis of variance unless otherwise indicated.

RESULTS

Identification of CRTC2 in the Pin1-containing Complex from Mouse Liver—The adenovirus to MEF-tagged Pin1 was introduced into mice, and the Pin1-containing complex was purified. Purified Pin1 in the complex was electrophoresed and subjected to silver staining, which showed the presence of Pin1 bait proteins and many binding proteins (Fig. 1*A*). Bands (1), (2), and (3) were identified to be DNA-directed RNA polymerase II A, DNA-directed RNA polymerase IIB, and DNA-directed RNA polymerase I by the analysis using LC/MS, which agree with previous reports (23). Then we performed the immunoblotting using many antibodies to detect another protein included in the Pin1-containing complex because many faint bands were visible with silver staining.

Many transcriptional co-activators are included among the target proteins of Pin1 (4, 5). In addition, although one of the regulatory mechanisms of Pin1 is protein stabilization, recent reports have shown that Pin1 is involved in translocation of target proteins, such as Bax (24). These results suggest that CRTC2 is a candidate Pin1 target protein because CRTC2 is a transcriptional co-activator and is translocated between the cytosol and the nucleus. As a result, immunoblotting using anti-CRTC2 antibody indicated the presence of CTRC2 in the Pin1 complexes (Fig. 1*B*). To confirm the association between CTRC2 and Pin1, CRTC2 and each GFP-Pin1 or GFP were simultaneously overexpressed in HepG2 and Sf9 cells. As shown in Fig. 1*C* and supplemental Fig. 1, GFP-Pin1, but not GFP alone was detected in the anti-CRTC2 immunoprecipitate. Furthermore, CRTC2 was detected in the immunoprecipitate with anti-Pin1 antibody but not that with the control IgG from mouse liver (Fig. 1*D*). Thus, the association between CRTC2 and Pin1 is physiological.

Pin1 possesses the WW and PPIase domains in its N terminus (amino acids 1–38) and C terminus (amino acids 39–163), respectively. To identify the domain of Pin1 responsible for the association with CRTC2, we prepared GST-Pin1, the GST-Pin1 WW domain, and the GST-Pin1 PPIase domain. These GST proteins were conjugated to beads, followed by incubation with cell lysates from MEF-tagged CRTC2 overexpressing HepG2 cells. GST-Pin1 but not GST alone bound to CRTC2 *in vitro* (Fig. 1*E*). Using this pull-down system, it was shown that the GST-WW domain, but not the GST-PPIase domain, binds to CRTC2 (Fig. 1*F*). In addition, okadaic acid treatment significantly increased the association of CRTC2 with Pin1 (Fig. 1*G*),

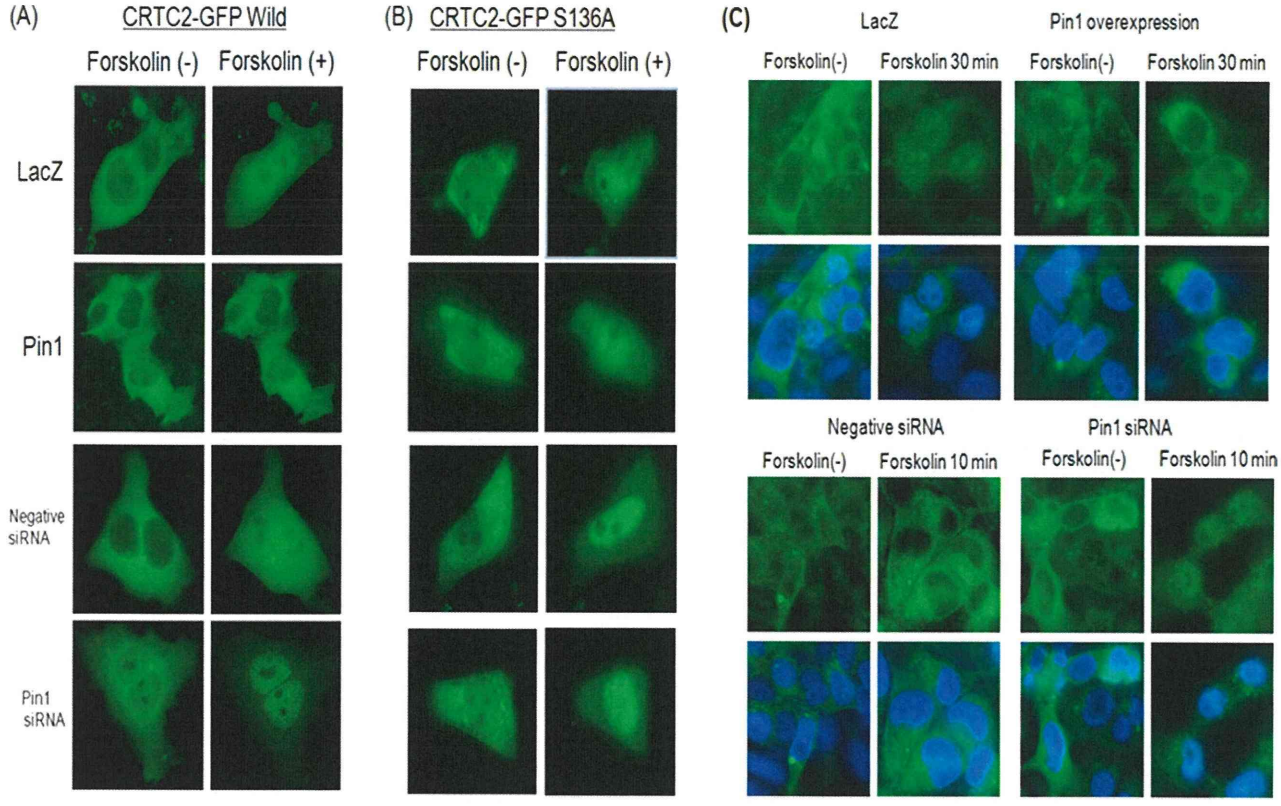

FIGURE 3. **Effect of Pin1 on subcellular localization of GFP-tagged CRTC2.** *A* and *B*, LacZ or Pin1 was overexpressed, or HepG2 cells were treated with control or Pin1 siRNAs. Then GFP-tagged CRTC2 was overexpressed in HepG2 cells. These cells were treated with forskolin, and the subcellular localization of GFP-tagged wild type or S136A CRTC2 was examined at the indicated periods after initiating forskolin stimulation. Representative data from four independent experiments are shown. *C*, LacZ or Pin1 was overexpressed in HepG2 cells, or the cells were treated with control or Pin1 siRNAs. These cells were treated with forskolin, and the subcellular localization of endogenous CRTC2 was determined by immunostaining at 10 or 30 min after initiating forskolin stimulation. Nuclei were stained with DAPI. Representative data from five independent experiments are shown.

suggesting the involvement of serine and/or threonine phosphorylation(s) in CRTC2.

Pin1 Associates with Ser^{136}-containing Motif in the NLS Domain of CRTC2—Subsequently, to reveal the domain of CRTC2 responsible for the association with Pin1, six Ds-Red-tagged CRTC2 N terminus deletion mutants (Fig. 2*A*) and GFP-tagged Pin1 were simultaneously overexpressed in Sf9 cells. As shown in Fig. 2*B*, CRTC2 deletion mutant 2 (D-2), containing amino acids 121–238, was immunoprecipitated with GFP-tagged Pin1 but not with GFP alone. This portion contains three serine-proline motifs (Fig. 2*C*). Each of these serine residues was replaced with alanine, creating a mutant that did not associate with Pin1. As shown in Fig. 2*D*, CRTC2 with serine 136 replaced by alanine did not bind to Pin1, whereas CRTC with serine 129 or 131 bound to Pin1 (data not shown). These observations indicated that the association between CRTC2 and Pin1 is mediated via the phosphoserine 136-containing motif in CRTC2 and the WW domain in Pin1. Ser^{136} is in the NLS domain, and a high level of Ser^{136} phosphorylation was demonstrated in a previous report (16).

Pin1 Inhibits CRTC2 Translocation from the Cytosol to the Nucleus—To test whether or not the effect of Pin1 on CRE transcriptional activity is mediated via the effect on the subcellular localization of CRTC2, the GFP-tagged CRTC2 was overexpressed, and the effects of the Pin1 expression level on the subcellular localization of GFP-tagged CRTC2 were analyzed in the absence or presence of forskolin stimulation (Fig. 3*A*). In the control LacZ-overexpressing or control siRNA-treated HepG2 cells, GFP-tagged CRTC2 was translocated from the cytosol to the nucleus, as reported previously (9). Pin1 overexpression markedly inhibited forskolin-induced translocation of CRTC2 into the nucleus. In addition, gene silencing of Pin1 using siRNA markedly enhanced the nuclear translocation of Pin1 in comparison with treatment with control siRNA. Although nuclear CRTC2 S136A (unable to bind to Pin1) was required for forskolin stimulation, it had no effect on either Pin1 overexpression or Pin1 siRNA (Fig. 3*B*).

In addition, we investigated the effect of Pin1 on the distribution of CRTC2 S171A. CRTC2 S171A (unable to bind to 14-3-3) was mainly present in the nucleus regardless of forskolin stimulation (supplemental Fig. 2). Pin1 overexpression slightly increased CRTC2 S171A in the cytosol, whereas Pin1 siRNA treatment reduced the amount of CRTC2 S171A in the cytosol. This effect of Pin1 was essentially in agreement with the results obtained for wild-type CRTC2.

Similar results were obtained by immunostaining the endogenous CRTC2 in HepG2 cells (Fig. 3*C*). Pin1 overexpression attenuated the forskolin-induced nuclear translocation of CRTC2 as compared with LacZ overexpression. On the other hand, treatment with Pin1 siRNA increased CRTC2 in the nucleus under forskolin stimulation as compared with the control siRNA.

Neither the distribution nor the expression of Pin1 was changed by forskolin or insulin stimulation (supplemental Fig. 3). Thus, a change in Pin1 is not required for regulation of the CRTC2 distribution.

Pin1 Associates with CRTC1 and Induces Its Localization in the Cytosol—The CRTC family consists of three isoforms, CRTC1, CRTC2, and CRTC3. The motif of CRTC2 responsible for the association with Pin1 is present in the NLS and is conserved in CRTC1 but not in CRTC3 (supplemental Fig. 4*A*). Thus, the associations of Pin1 with CRTC1 were also investigated using HepG2 cells. As shown in supplemental Fig. 4*B*, FLAG-tagged CRTC1 was detected in anti-GFP immunoprecipitates from the cells expressing GFP-tagged Pin1 and FLAG-tagged CRTC1. As shown in supplemental Fig. 4*C*, FLAG-tagged CRTC1, in which serine 155 is replaced with alanine, did not bind to GFP-tagged Pin1, unlike the FLAG-tagged wild-type CRTC1.

Then the effects of Pin1 on localizations of CRTC1 were examined. When LacZ was overexpressed, GFP-tagged CRTC1 was present in the cytosol and translocated to the nucleus in response to forskolin stimulation (supplemental Fig. 4*D*). This translocation was markedly inhibited by Pin1 overexpression (supplemental Fig. 4*D*).

CRTC2 Associated with Pin1 Did Not Bind to CREB—Formation of the CREB·CBP·CTRC complex, which binds to a CRE site, is critical for CRE transcriptional activation. We investigated whether or not the CREB·CBP·CRTC2·Pin1 complex can form, using the baculovirus and Sf9 cell overexpression system. When CRTC2 and CREB were both overexpressed in HepG2 or Sf9 cells, CREB was detected in the CRTC2 immunoprecipitate. Interestingly, the overexpression of Pin1 markedly reduced the association between CREB and CRTC2, in either HepG2 or Sf9 cells (Fig. 4, *A* and *B*).

Furthermore, the effect of Pin1 on the association between CRTC2 and 14-3-3 was investigated. In Sf9 cell lysates overexpressing CREB and CRTC2, both CRTC2 and endogenously expressed 14-3-3 protein were detected in anti-CREB immunoprecipitates (Fig. 4*C*). In the case of triple overexpressions of CRTC2, CREB, and GFP-tagged Pin1, CRTC2 and 14-3-3 were detectable in the GFP-tagged Pin1 immunoprecipitate (Fig. 4*D*).

Similar results were obtained in the HepG2 cells. The association between MEF-tagged CRTC2 and endogenously expressed 14-3-3 was not affected by the overexpression of Pin1 (supplemental Fig. 5*A*). In addition, Pin1 overexpression did not affect the phosphorylation level of Ser^{171}, responsible for the association with 14-3-3, in either basal or forskolin-stimulated conditions (supplemental Fig. 5*B*). These results suggest that Pin1-associated CRTC2 is capable of binding to 14-3-3 protein but not to CREB.

Pin1 Inhibits CRE Transcriptional Activity and Its Downstream PEPCK Expression—Subsequently, to elucidate the role of Pin1 in CRE transcriptional activity, the effects of Pin1 overexpression and Pin1 gene silencing using siRNA on the CRE and PEPCK luciferase assay, and PEPCK mRNA level were investigated in HepG2 cells (Fig. 5). The amount of overexpressed Pin1 was ~5 times that of endogenous Pin1 in HepG2 cells. Under these conditions, forskolin-induced transcriptional activity and PEPCK mRNA induction were significantly attenuated (Fig. 5, *A–C*). On the contrary, gene suppression of Pin1 using siRNA significantly enhanced these events (Fig. 5, *D–F*). In addition, suppressions of CRE-luciferase and PEPCK-luciferase activities by Pin1 overexpression were observed in immortalized human hepatocytes (supplemental Fig. 6) (25), suggesting that this mechanism is independent of the glucose sensitivity of the cell type. An inhibitory effect of Pin1 on CRE luciferase activity was observed when wild type or S171A CRTC2, but not S136A, was overexpressed, consistent with the results showing Pin1 to regulate the translocation of CRTC2 (supplemental Fig. 7). Thus, the Pin1 expression level was revealed to negatively regulate CRE transcriptional activity.

Chromatin Immunoprecipitation Assay with Anti-CRTC2 and CREB Antibodies—Because Pin1-associated CRTC2 did not bind CREB, we performed a ChIP assay to investigate whether or not Pin1 affected recruitment of CRTC2 to cAMP-responsive elements upstream of PEPCK, NR4A2, and CGA genes (Fig. 5*G*). The PCR product obtained using the anti-CREB immunoprecipitate was unchanged regardless of forskolin stimulation or Pin1 overexpression. In contrast, the PCR product of the anti-CRTC2 immunoprecipitate was markedly increased by forskolin stimulation, and Pin1 overexpression abolished this increase. Forskolin stimulation induced CBP recruitment to the promoter as well as CRTC2, but Pin1 overexpression had no effect.

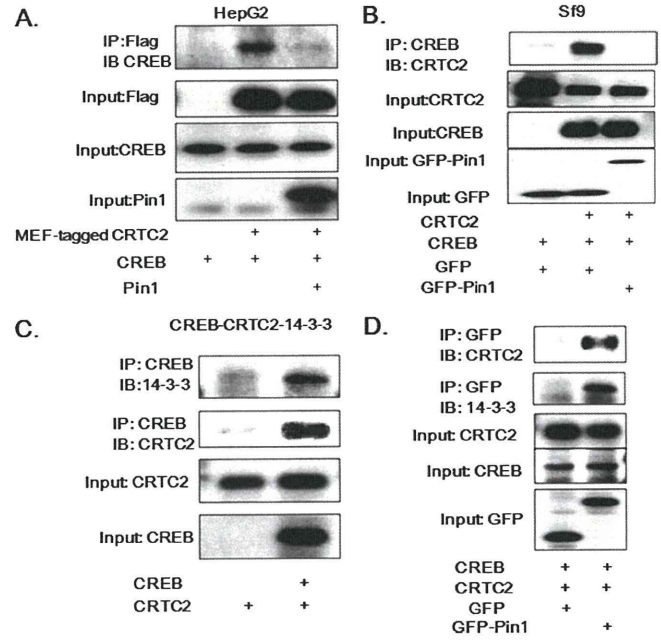

FIGURE 4. **Binding of Pin1 to CRTC2 inhibits the association between CREB and CRTC2 but not that between 14-3-3 and CRTC2.** *A*, MEF-tagged CRTC2, CREB, and Pin1 were overexpressed in HepG2 cells in the indicated combinations. The cell lysates were immunoprecipitated (*IP*) with anti-FLAG antibody and immunoblotted (*IB*) with anti-CREB antibody. *B*, CRTC2, CREB, and Pin1 were overexpressed in Sf9 cells in the indicated combinations. The cell lysates were immunoprecipitated with anti-CREB antibody and immunoblotted with anti-CRTC2 antibody. *C*, CREB and CRTC2 were overexpressed in Sf9 cells. The cell lysates were immunoprecipitated with anti-CREB antibody and immunoblotted with anti-14-3-3 protein antibody. *D*, CREB, CRTC2, and either GFP or GFP-Pin1 were overexpressed in Sf9 cells. The cell lysates were immunoprecipitated with anti-GFP antibody and immunoblotted with anti-CRTC2 or anti-14-3-3 protein antibody. Representative data from four independent experiments are shown.

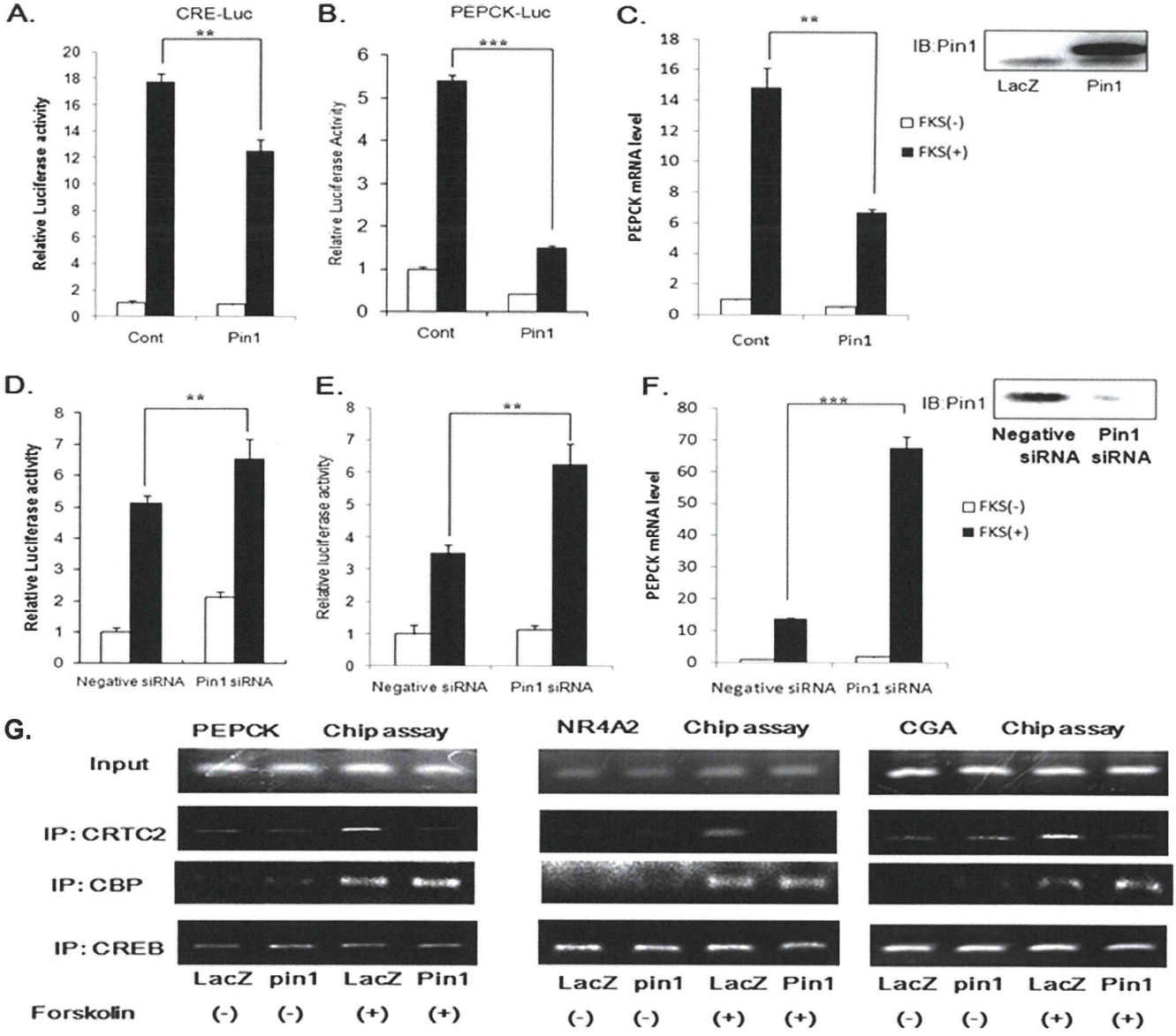

FIGURE 5. **Pin1 suppresses CRE luciferase activity and PEPCK mRNA level in HepG2 cells.** *A* and *B*, LacZ or Pin1 was overexpressed in HepG2 cells transfected with pTAL and pTAL-CRE or pTAL-PEPCK. *D* and *E*, these transfected HepG2 cells were treated with control siRNA or Pin1 siRNA. In two experiments, with and without forskolin stimulation for 6 h, the cell lysates from HepG2 cells were subjected to the luciferase assay. *C* and *F*, PEPCK mRNA levels were also measured. Representative data from four independent experiments are shown. **, $p < 0.01$ *versus* LacZ or negative siRNA. *G*, HepG2 cells overexpressing LacZ or Pin1 were subjected to the CHIP assay using anti-CRTC2, anti-CNP, or anti-CREB antibodies and primers corresponding to the PEPCK, NR4A2, and CGA promoter regions. Representative data from four independent experiments are shown. *IB*, immunoblot; *IP*, immunoprecipitation. *Error bars*, S.E.

Thus, it was suggested that CRTC2 associated with Pin1 was removed from CREB located in the CRE sequence in the PEPCK, NR4A2, and CGA promoter region.

Hepatic Pin1 Overexpression Reduces PEPCK Expression and Decreases Hyperglycemia in STZ-induced Diabetic Mice—CRTC2 is a major transcriptional co-activator for hepatic glucose regulation via its effects on PEPCK expression. Thus, we considered the possibility of the regulation of PEPCK expression by Pin1 in the liver, and an adenovirus expressing Pin1 was introduced into STZ-induced insulin-deficient diabetic mice. Due to the insulin deficiency, as reported previously, hepatic PEPCK mRNA and serum blood glucose levels were markedly increased in fed and fasted state, as compared with the control mice (Fig. 6). The adenovirus for Pin1 expression was injected intravenously, and 96 h later, overexpressed Pin1 was detected only in the liver (Fig. 6*A*) and not in other tissues. With Pin1 overexpression in the liver, the increased hepatic PEPCK mRNA level in STZ-mice was normalized, and blood glucose elevation was also partially but significantly reduced in both the fed and the fasting state (Fig. 6, *B–E*). Pin1 overexpression exerted the same effects on other CRE-dependent transcriptional genes, such as G6Pase, PGC-1a, and CPT-1. These findings revealed Pin1 to be a regulator of CRE-dependent transcriptional genes *in vivo*.

Pin1 Expression Is Low in Fasting State—Finally, we investigated the changes in Pin1 expressions under different nutrient condi-

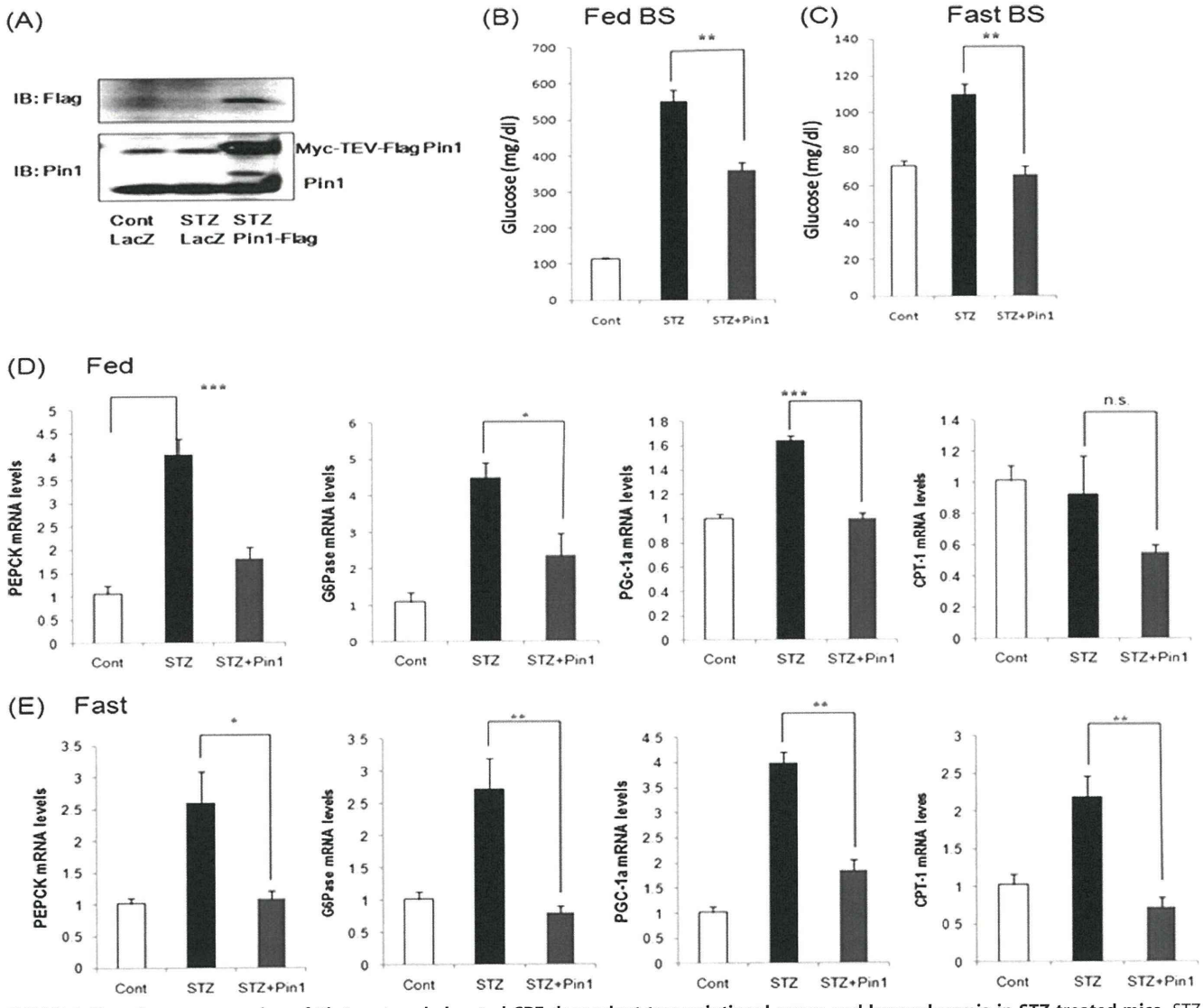

FIGURE 6. **Hepatic overexpression of Pin1 restored elevated CRE-dependent transcriptional genes and hyperglycemia in STZ-treated mice.** STZ-treated diabetic C57BL/6 male mice were injected with 2.5×10^7 plaque-forming units/g body weight of adenovirus containing β-galactosidase (*LacZ*) or FLAG-tagged Pin1 construct via the tail vein. *A*, immunoblotting of hepatic tissue lysates with anti-FLAG or anti-Pin1 antibody. *B* and *C*, serum glucose concentrations in fed and fasting states ($n = 6$, each group). *D* and *E*, CRE-dependent transcriptional gene mRNA levels in the liver. **, $p < 0.01$ *versus* STZ; ***, $p < 0.001$ *versus* STZ. *Error bars*, S.E.

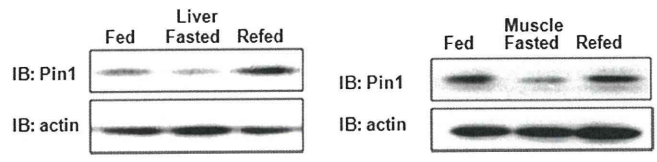

FIGURE 7. **Pin1 expression is regulated by nutrient conditions.** Mice were fed routinely, starved for 20 h, or refed for 4 h after a 20-h fast. Liver (*left*) and muscle (*right*) cell lysates were prepared and then immunoblotted with anti-Pin1 antibody. A representative immunoblot (*IB*) is shown in the *upper panel*.

tions. Interestingly, we found that the Pin1 expression level is low in the fasted state but is increased by feeding (Fig. 7). Thus, Pin1 expression appears to be regulated by nutrient conditions.

DISCUSSION

CRE transcriptional activity is enhanced through association of the CREB·CBP·CRTC complex on a CRE site. The co-activator of CREB termed the CRTC family consists of three isoforms, CRTC1, CRTC2, and CRTC3 (18). CRTC2 was reported to be important for the regulation of CRE transcriptional activity and its downstream PEPCK gene expression (20). Depletion of nuclear CRTC2 leads to the suppression of CRE transcriptional activity (20). Thus, both the subcellular localization of CRTC2 and CREB·CBP·CRTC complex formation are critical for CRE transcriptional activity. CRTC2 is reportedly phosphorylated by AMPK and SIK, and phosphorylated CRTC2 binds to 14-3-3 protein and is thereby shifted from the nucleus to the cytoplasm (21). The Montiminy group (16) has identified 12 independent phosphorylated serine residues on CRTC2 using tandem MS analysis. They demonstrated that PKA inhibits the activity of SIK and reduces Ser^{171} phosphorylation leading to binding with 14-3-3 protein and translocation to the cytosol (16). However, the importance of other phosphorylation sites identified in their study, such as Ser^{136} remains unknown.

In this study, it was demonstrated that Pin1 associates with the CRTC family of proteins consisting of CRTC1 and CRTC2. Because the portion of CRTC1 and CRTC2 responsible for the association with Pin1 is in the NLS domain, we considered the possibility that the binding of Pin1 to this portion would interrupt NLS function, resulting in their export from the nucleus. In fact, our observations using GFP-tagged CRTC1 and CRTC2 as well as staining of endogenous CRTC2 supported our hypothesis. On the other hand, gene silencing of Pin1 using siRNA markedly induced nuclear localization of CRTC2 when stimulated with forskolin. It is likely that altered localization of CTRC2 due to Pin1 takes place independently of the binding of 14-3-3 protein to CRTC2 because Pin1 overexpression affected neither the Ser^{171} phosphorylation level of CRTC2 nor the association with 14-3-3.

A further interesting issue is that CRTC2 associated with Pin1 did not bind to CREB. This phenomenon cannot be attributable to the different subcellular distributions of CREB, CBP, and CRTC because highly overexpressed CREB, CBP, and CRTC2 are present in the cytosol of Sf9 cells. Taken together, these observations indicate the association of Pin1 with CRTC2 to decrease the nuclear CBP·CRTC2·CREB complex via two mechanisms (*i.e.* the export of CRTC2 and interruption of the association between CRTC2 and CREB). Thus, the Pin1 expression level is a key factor regulating CRE transcriptional activity.

We investigated the effects of various kinase inhibitors on the association between CRTC2 and Pin1, using HepG2 cells, in an effort to identify the kinase that is involved in the phosphorylation of S136A on CRTC2. However, we were unable to obtain clear results. Although we did not discover which kinase(s) phosphorylates the Ser^{136} of CRTC2 responsible for the association with Pin1 in this study, high basal phosphorylation of Ser^{136} was already demonstrated in a previous report (16).

Prior studies have also shown that Pin1 expression generally correlates with cell proliferative potential in normal tissues (1, 26, 27) and is further up-regulated in many human cancers (28–31). In addition, interestingly, we noticed that the amount of Pin1 was higher in the fed than in the fasting state, in both liver and muscle. However, neither insulin nor forskolin has any effect on the expression of Pin1 in HepG2. Thus, the mechanism(s) involved in the altered expression of Pin1 remains unclear, although this is an important issue that merits further investigation.

In the liver, CRE transcriptional activity plays a critical role in gluconeogenesis (32–34). In addition, in the diabetic state, insufficient suppression of CRE transcriptional activity is regarded as a mechanism underlying hyperglycemia under fasted conditions (35). In the present study, our final experiment examined whether Pin1 overexpression might improve the hyperglycemia in insulin-deficient STZ-treated mice. In these mice, gluconeogenic enzymes, such as PEPCK, under the control of CRE transcriptional activity are reportedly up-regulated (20, 36, 37) due to insulin deficiency and the relatively increased effect of glucagon. The fact that Pin1 overexpression reduced the high PEPCK expression and its resultant fasting serum glucose elevation in STZ-treated mice suggests that the Pin1 expression level is involved in regulating glucose metabolism. Thus, an agent affecting Pin1 expression or activity may represent a novel therapeutic strategy for diabetes.

To date, numerous proteins have been identified as substrates of Pin1 (4, 5, 38). With the proline conformational change induced by Pin1, the structure and function of the target protein are modified, which affects protein stabilization, subcellular localization, phosphorylation, transcriptional activity, etc. In the case of CTRC2, both subcellular localization and the complex-forming function with CREB are affected.

Although we did not investigate the physiological effects occurring via CRTC1 induced by the association with Pin1, we did observe that Pin1 is highly expressed in the brain, whereas its enzymatic activity is blunted by oxidative stress modification that occurs in the early stages of Alzheimer disease (39). Although the physiological function of Pin1 in neurons remains largely unknown, numerous reports have implicated CRE transcriptional activity in brain function (40–42). Thus, further important evidence may be obtained from studies of Pin1 and CRTC1 in the brain or other tissues.

In summary, CRTC2 was identified as a new Pin1-binding protein. The CBP·CRTC2·CREB complex promotes gluconeogenesis. Pin1 binding to CRTC2 prevents this complex formation, thereby suppressing CRE transcriptional activity (supplemental Fig. 8). These findings indicate that Pin1 is a regulator of gluconeogenesis and may be a new target for diabetic therapy.

REFERENCES

1. Lu, K. P., Hanes, S. D., and Hunter, T. (1996) *Nature* **380,** 544–547
2. Lu, P. J., Wulf, G., Zhou, X. Z., Davies, P., and Lu, K. P. (1999) *Nature* **399,** 784–788
3. Pinton, P., Rimessi, A., Marchi, S., Orsini, F., Migliaccio, E., Giorgio, M., Contursi, C., Minucci, S., Mantovani, F., Wieckowski, M. R., Del Sal, G., Pelicci, P. G., and Rizzuto, R. (2007) *Science* **315,** 659–663
4. Takahashi, K., Uchida, C., Shin, R. W., Shimazaki, K., and Uchida, T. (2008) *Cell Mol. Life Sci.* **65,** 359–375
5. Wulf, G., Finn, G., Suizu, F., and Lu, K. P. (2005) *Nat. Cell Biol.* **7,** 435–441
6. Ranganathan, R., Lu, K. P., Hunter, T., and Noel, J. P. (1997) *Cell* **89,** 875–886
7. Schutkowski, M., Bernhardt, A., Zhou, X. Z., Shen, M., Reimer, U., Rahfeld, J. U., Lu, K. P., and Fischer, G. (1998) *Biochemistry* **37,** 5566–5575
8. Bittinger, M. A., McWhinnie, E., Meltzer, J., Iourgenko, V., Latario, B., Liu, X., Chen, C. H., Song, C., Garza, D., and Labow, M. (2004) *Curr. Biol.* **14,** 2156–2161
9. Dentin, R., Hedrick, S., Xie, J., Yates, J., 3rd, and Montminy, M. (2008) *Science* **319,** 1402–1405
10. He, L., Sabet, A., Djedjos, S., Miller, R., Sun, X., Hussain, M. A., Radovick, S., and Wondisford, F. E. (2009) *Cell* **137,** 635–646
11. Herzig, S., Long, F., Jhala, U. S., Hedrick, S., Quinn, R., Bauer, A., Rudolph, D., Schutz, G., Yoon, C., Puigserver, P., Spiegelman, B., and Montminy, M. (2001) *Nature* **413,** 179–183
12. Jansson, D., Ng, A. C., Fu, A., Depatie, C., Al Azzabi, M., and Screaton, R. A. (2008) *Proc. Natl. Acad. Sci. U.S.A.* **105,** 10161–10166
13. Lerner, R. G., Depatie, C., Rutter, G. A., Screaton, R. A., and Balthasar, N. (2009) *EMBO Rep.* **10,** 1175–1181
14. Liu, Y., Dentin, R., Chen, D., Hedrick, S., Ravnskjaer, K., Schenk, S., Milne, J., Meyers, D. J., Cole, P., Yates, J., 3rd, Olefsky, J., Guarente, L., and Montminy, M. (2008) *Nature* **456,** 269–273
15. Radhakrishnan, I., Pérez-Alvarado, G. C., Parker, D., Dyson, H. J., Montminy, M. R., and Wright, P. E. (1997) *Cell* **91,** 741–752
16. Screaton, R. A., Conkright, M. D., Katoh, Y., Best, J. L., Canettieri, G., Jeffries, S., Guzman, E., Niessen, S., Yates, J. R., 3rd, Takemori, H., Okamoto, M., and Montminy, M. (2004) *Cell* **119,** 61–74

17. Zhou, X. Y., Shibusawa, N., Naik, K., Porras, D., Temple, K., Ou, H., Kaihara, K., Roe, M. W., Brady, M. J., and Wondisford, F. E. (2004) *Nat. Med.* **10,** 633–637
18. Iourgenko, V., Zhang, W., Mickanin, C., Daly, I., Jiang, C., Hexham, J. M., Orth, A. P., Miraglia, L., Meltzer, J., Garza, D., Chirn, G. W., McWhinnie, E., Cohen, D., Skelton, J., Terry, R., Yu, Y., Bodian, D., Buxton, F. P., Zhu, J., Song, C., and Labow, M. A. (2003) *Proc. Natl. Acad. Sci. U.S.A.* **100,** 12147–12152
19. Wu, Z., Huang, X., Feng, Y., Handschin, C., Feng, Y., Gullicksen, P. S., Bare, O., Labow, M., Spiegelman, B., and Stevenson, S. C. (2006) *Proc. Natl. Acad. Sci. U.S.A.* **103,** 14379–14384
20. Dentin, R., Liu, Y., Koo, S. H., Hedrick, S., Vargas, T., Heredia, J., Yates, J., 3rd, and Montminy, M. (2007) *Nature* **449,** 366–369
21. Koo, S. H., Flechner, L., Qi, L., Zhang, X., Screaton, R. A., Jeffries, S., Hedrick, S., Xu, W., Boussouar, F., Brindle, P., Takemori, H., and Montminy, M. (2005) *Nature* **437,** 1109–1111
22. Sakoda, H., Gotoh, Y., Katagiri, H., Kurokawa, M., Ono, H., Onishi, Y., Anai, M., Ogihara, T., Fujishiro, M., Fukushima, Y., Abe, M., Shojima, N., Kikuchi, M., Oka, Y., Hirai, H., and Asano, T. (2003) *J. Biol. Chem.* **278,** 25802–25807
23. Xu, Y. X., and Manley, J. L. (2007) *Genes Dev.* **21,** 2950–2962
24. Shen, Z. J., Esnault, S., Schinzel, A., Borner, C., and Malter, J. S. (2009) *Nat. Immunol.* **10,** 257–265
25. Tontonoz, P., Hu, E., Devine, J., Beale, E. G., and Spiegelman, B. M. (1995) *Mol. Cell. Biol.* **15,** 351–357
26. Waki, K., Anno, K., Ono, T., Ide, T., Chayama, K., and Tahara, H. (2010) *Cancer Sci.* **101,** 1678–1685
27. Winkler, K. E., Swenson, K. I., Kornbluth, S., and Means, A. R. (2000) *Science* **287,** 1644–1647
28. Ryo, A., Nakamura, M., Wulf, G., Liou, Y. C., and Lu, K. P. (2001) *Nat. Cell Biol.* **3,** 793–801
29. Wulf, G. M., Ryo, A., Wulf, G. G., Lee, S. W., Niu, T., Petkova, V., and Lu, K. P. (2001) *EMBO J.* **20,** 3459–3472
30. Yeh, E., Cunningham, M., Arnold, H., Chasse, D., Monteith, T., Ivaldi, G., Hahn, W. C., Stukenberg, P. T., Shenolikar, S., Uchida, T., Counter, C. M., Nevins, J. R., Means, A. R., and Sears, R. (2004) *Nat. Cell Biol.* **6,** 308–318
31. Zheng, H., You, H., Zhou, X. Z., Murray, S. A., Uchida, T., Wulf, G., Gu, L., Tang, X., Lu, K. P., and Xiao, Z. X. (2002) *Nature* **419,** 849–853
32. Erion, D. M., Ignatova, I. D., Yonemitsu, S., Nagai, Y., Chatterjee, P., Weismann, D., Hsiao, J. J., Zhang, D., Iwasaki, T., Stark, R., Flannery, C., Kahn, M., Carmean, C. M., Yu, X. X., Murray, S. F., Bhanot, S., Monia, B. P., Cline, G. W., Samuel, V. T., and Shulman, G. I. (2009) *Cell Metab.* **10,** 499–506
33. Rhee, J., Inoue, Y., Yoon, J. C., Puigserver, P., Fan, M., Gonzalez, F. J., and Spiegelman, B. M. (2003) *Proc. Natl. Acad. Sci. U.S.A.* **100,** 4012–4017
34. Rodgers, J. T., Lerin, C., Haas, W., Gygi, S. P., Spiegelman, B. M., and Puigserver, P. (2005) *Nature* **434,** 113–118
35. Yoon, J. C., Puigserver, P., Chen, G., Donovan, J., Wu, Z., Rhee, J., Adelmant, G., Stafford, J., Kahn, C. R., Granner, D. K., Newgard, C. B., and Spiegelman, B. M. (2001) *Nature* **413,** 131–138
36. Clément, S., Krause, U., Desmedt, F., Tanti, J. F., Behrends, J., Pesesse, X., Sasaki, T., Penninger, J., Doherty, M., Malaisse, W., Dumont, J. E., Le Marchand-Brustel, Y., Erneux, C., Hue, L., and Schurmans, S. (2001) *Nature* **409,** 92–97
37. Fisher, S. J., and Kahn, C. R. (2003) *J. Clin. Invest.* **111,** 463–468
38. Ryo, A., Suizu, F., Yoshida, Y., Perrem, K., Liou, Y. C., Wulf, G., Rottapel, R., Yamaoka, S., and Lu, K. P. (2003) *Mol Cell.* **12,** 1413–1426
39. Sultana, R., Boyd-Kimball, D., Poon, H. F., Cai, J., Pierce, W. M., Klein, J. B., Markesbery, W. R., Zhou, X. Z., Lu, K. P., and Butterfield, D. A. (2006) *Neurobiol. Aging* **27,** 918–925
40. Bito, H., Deisseroth, K., and Tsien, R. W. (1996) *Cell* **87,** 1203–1214
41. Nibuya, M., Nestler, E. J., and Duman, R. S. (1996) *J. Neurosci.* **16,** 2365–2372
42. Tao, X., Finkbeiner, S., Arnold, D. B., Shaywitz, A. J., and Greenberg, M. E. (1998) *Neuron* **20,** 709–726

Supplementary Figure.1 Pin1 associates with CRTC2 in Sf9

CRTC2 was over-expressed with GFP or GFP-Pin1. Then, the cell lysates were immunoprecipitated with anti-CRTC2 antibody, followed by immunoblotting with anti-GFP antibody.

Supplementary Figure.2 Effect of Pin1 on subcellular localization of GFP-tagged S171 A CRTC2

LacZ or Pin1 was over-expressed, or HepG2 cells were treated with control or Pin1 siRNAs. Then, GFP-tagged S171A CRTC2 was over-expressed in HepG2 cells. These cells were treated with forskolin and the subcellular localization of GFP-tagged S171A CRTC2 was examined at 30 min after initiating forskolin stimulation. Representative data from four independent experiments are shown.

Supplementary Figure 3 Effects of glucagon and insulin on Pin1 distribution and expression

(A, B) GFP-tagged Pin1 was over-expressed in HepG2 cells. These cells were treated with forskolin or insulin, and the subcellular localization of GFP-tagged Pin1 was examined at 30 min after stimulation. (C, D) HepG2 cells were suspended in Laemmli sample buffer 24 hr after forskolin or insulin stimulation, followed by Western blot analysis.

Supplementary Figure 4 Pin1 associates with CRTC1 and induces its translocation in the cytosol.

(A) Amino acid sequence alignment of the NLS domains of CRTC1, CRTC2 and CRTC3. The Ser-Pro motifs responsible for the association with Pin1 in CRTC1 and CRTC2 are in red. (B) FLAG-tagged CRTC1 or CRTC2 was over-expressed with GFP or GFP-Pin1 in HepG2 cells. Then, the cell lysates were immunoprecipitated with anti- FLAG antibody followed by immunoblotting with anti-GFP antibody. (C) Wild-type CRTC1 or CRTC1 S155A was over-expressed with GFP-Pin1 or GFP in HepG2 cells. The cell lysates were immunoprecipitated with anti-FLAG antibody followed by immunoblotting with anti-GFP. The upper panel shows that CRTC1 S155A does not associate with Pin1, unlike wild-type CRTC1. Representative data from five independent experiments are shown. (D) GFP-tagged CRTC1 were over-expressed in HeLa cells. Then, LacZ or Pin1 was over-expressed, and the cells were treated with or without forskolin. Subcellular localizations of GFP-tagged CRTC1 was examined. Representative data from five independent experiments are shown.

Supplementary Figure 5 Binding of Pin1 to CRTC2 did not affect the association

between CRTC2 and 14-3-3, and p-CRTC2 171Ser

(A, B) MEF-tagged CRTC2 and Pin1 were over-expressed in HepG2 cells in the indicated combinations. The cell lysates were immunoprecipitated with anti-CRTC2 antibody and immunoblotted with anti-14-3-3 antibody or pCRTC2 171S antibody

Supplementary Figure 6 Pin1 suppresses CRE and PEPCK luciferase activity in immortalized human hepatocytes

(A, B) LacZ or Pin1 was over-expressed in immortalized human hepatocytes transfected with pTAL and pTAL-CRE or pTAL-PEPCK. Then, the cell lysates were subjected to luciferase assay 24 hr after forskolin stimulation. $^{*}P<0.05$

Supplementary Figure 7 Effect of Pin1 on wild or mutant CRTC2-induced CRE luciferase activity Various CRTC2 and Pin1 were over-expressed in HepG2 cells transfected with pTAL and pTAL-CRE. Then, the cell lysates were subjected to luciferase assay. $^{**}P<0.01$

Supplementary Figure.8 Scheme of CRTC2 regulation by Pin1

With glucagon or forskolin stimulation, a CBP-CRTC2-CREB complex forms and promotes gluconeogenesis (left). CRTC2 binding to Pin1 prevents this complex formation, thereby suppressing CRE transcriptional activity (right).